Metal complexes of flavonoids: their synthesis, characterization, and enhanced anti-oxidant and anti-cancer activities

Article

Accepted Version

Metal complexes of Flavonoids: Their synthesis, characterization, and enhanced anti-oxidant and anti-cancer activities

Mai Khater[1,2], Divyashree Ravishankar[1], Francesca Greco[1] and Helen M.I. Osborn[1]*

[1] School of Pharmacy, University of Reading, Whiteknights, Reading, RG6 6AD. UK

[2] Therapeutic Chemistry Department, Pharmaceutical and Drug Industries Research Division, National Research Centre, Cairo, Egypt.

Abstract

Flavonoids are polyphenolic compounds of natural origin. They are extensively studied within drug discovery programmes due to their wide ranging biological activities such as anti-microbial, anti-oxidant, anti-tumor, neuroprotective and cardioprotective properties. The ability of flavonoids to coordinate with metal atoms has provided new leads for drug discovery programmes, with better pharmacological activities and clinical profiles than the parent flavonoids. In this review, the enhanced anti-oxidant and anti-cancer activities of flavonoid metal complexes versus the parent flavonoids are discussed. Possible mechanisms of action for the metal complexes, such as DNA binding and apoptosis induction, are also presented alongside an overview of the synthesis of the metal complexes, and the different techniques used for their characterization.

Keywords

Flavonoid, metal, flavonoid metal complex, anti-oxidant, anti-cancer.

Introduction

Flavonoids are phytochemicals that are mainly found in tea, citrus fruit, berries, apples and legumes. Chemically, they are polyphenolic compounds with a C_6-C_3-C_6 ring system (**Figure 1**) and they are often found in esterified or glycosylated forms [1]. It was not until the 1990's that research on flavonoids witnessed significant progress, with the number of publications increasing by approximately 6-fold, from 524 in 1990 to 3147 in 2017. As a result it is now well established that flavonoids have a wide and diverse range of biological activities [2, 3] such as anti-viral [4-6], anti-bacterial [7-10], neuroprotective [11-13], cardioprotective [14, 15], anti-oxidant [16-18] and anti-cancer [3, 19, 20] properties.

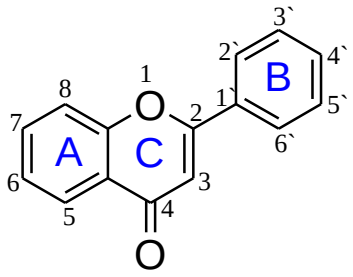

Basic skeleton of flavonoids

31

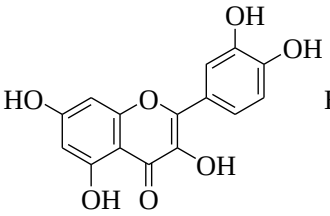

Quercetin

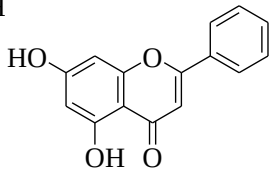

Chrysin

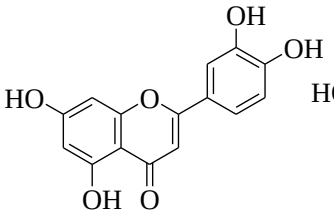

Luteolin

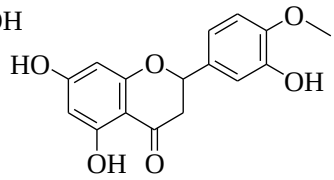

Hesperetin

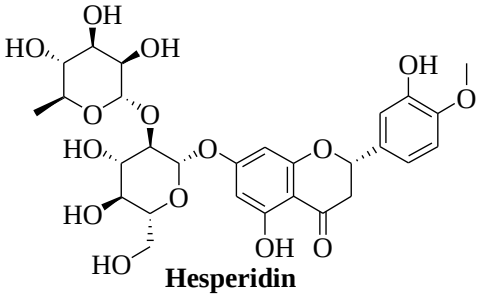

Hesperidin

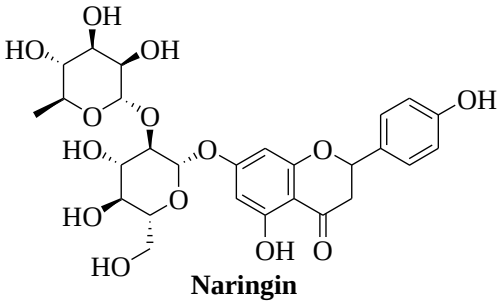

Naringin

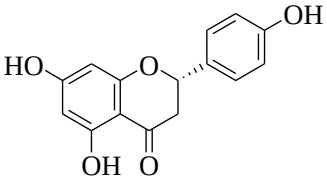

Naringenin

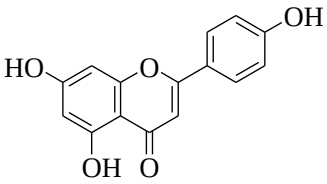

Apigenin

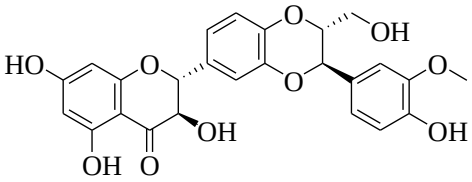

Silibinin

32

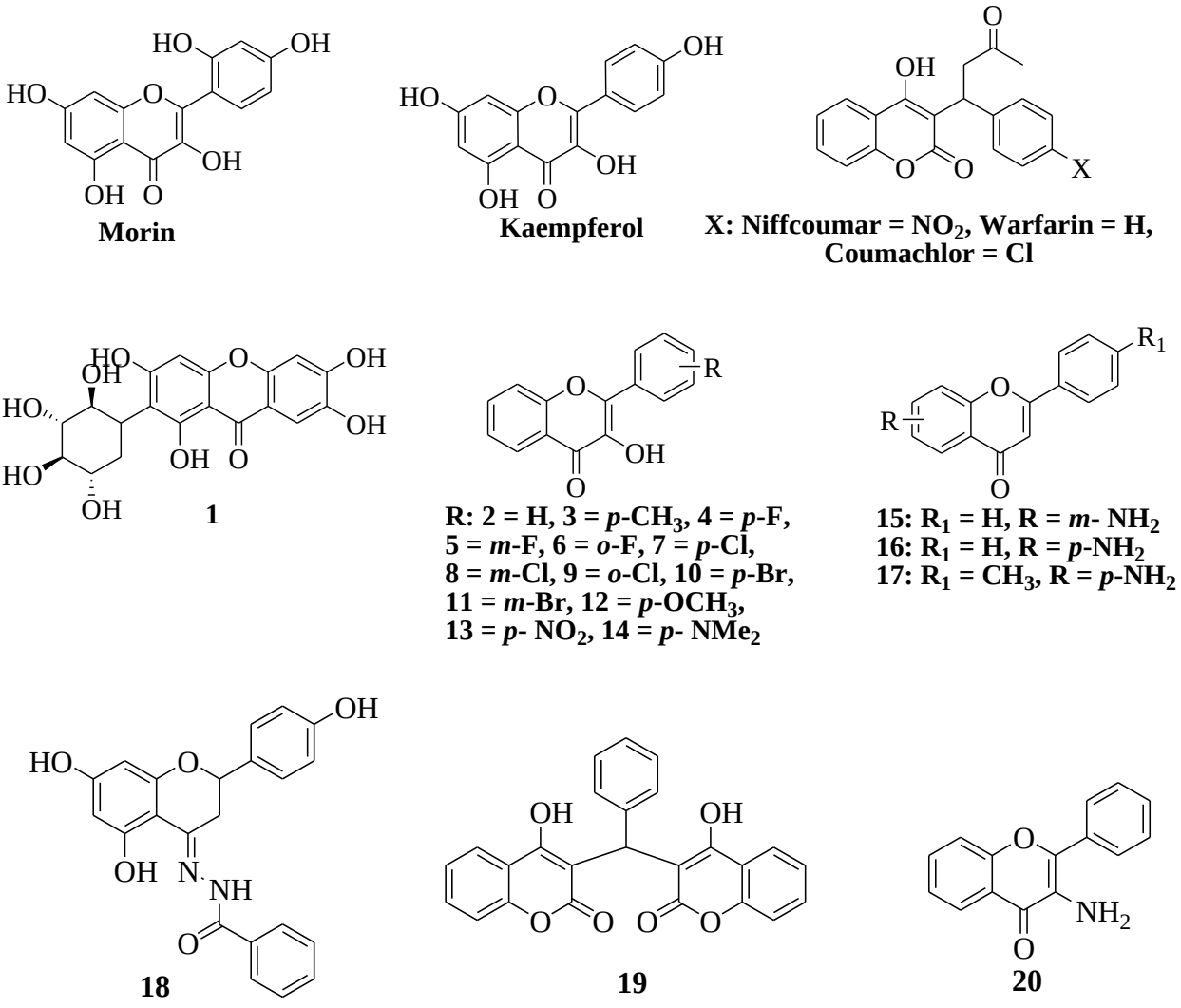

Figure 1. Chemical structures of flavonoids from which organometallic derivatives have been prepared

With respect to the beneficial health effects of flavonoids, the greatest impact has been seen within the anti-cancer field [2]. Flavonoids are known to interfere with an array of targets affecting cancer growth and progression. For example, they have been shown to induce cell cycle arrest and apoptosis [21] in addition to inhibiting mitotic spindle formation [22] and angiogenesis [23, 24]. Despite the advantages of having a compound that can interact with different targets, this can be a limitation due to limited selectivity. Indeed, this has been one of the biggest obstacles in the use of flavonoids as potential drugs due to its direct relation with adverse effects and poor *in vivo* toxicity profiles. However, despite the extensive research and number of structures and the activity reported for them, no flavonoid has to date reached the

market and only a limited number are in clinical investigation as anti-cancer agents, eg flavopiridol (phase-II) [25, 26], silibinin (phase-II) [27, 28], quercetin (phase-II) [29, 30] and the quercetin derivative QC12 (phase-I) [31] (**Figure 2**). Arguably, the main drug development challenge is the poor bioavailability of flavonoids, resulting from water insolubility and susceptibility to glucourinidation and/or methylation by intestinal and liver metabolism (first pass effect). There are several studies on the pharmacokinetics of flavonoids indicating their poor bioavailabilities. Wu et al., for instance, reported the absolute oral bioavailability of silibinin in rats to be approximately 0.95% [32]. In another study, flavopiridol's mean oral bioavailability following bolus intra-gavage was shown to be 20% [33]. Moreover, a study by Gugler et al. failed to detect any plasma quercetin concentrations in subjects receiving 4 g orally [34].

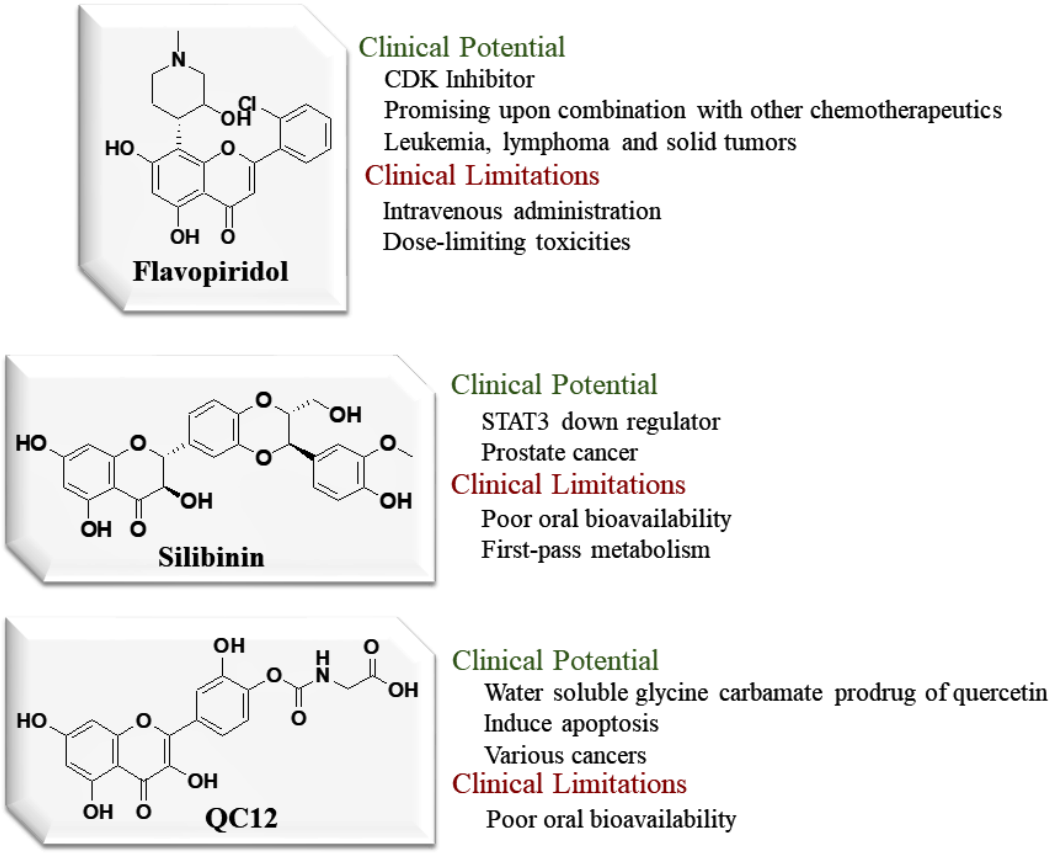

Figure 2. Flavonoids in clinical trials as anti-cancer agents

Due to the presence of hydroxyl and oxo groups within flavonoids, they possess metal chelating abilities that can have profound effects on their pharmacokinetic and pharmacological properties [35, 36]. The flavonoid structure, type of chelating metal and the pH of the surrounding medium

are determining factors of the preferred coordination site [37]. Metal atoms have beneficial biological properties such as chelating free radicals and binding to DNA [38]. These properties can cause synergistic effects when combined with other active chemical entities such as the flavonoids. Accordingly, metal complexation is reported to enhance the anti-oxidant, anti-proliferative and chemical properties of parent flavonoids. This review will therefore highlight important advances within the field of metal-flavonoid complexes with particular emphasis on their synthesis, methods of characterization, anti-oxidant and anti-proliferative activities.

Synthesis and characterization of flavonoid metal complexes

Flavonoid metal complexes are generally synthesized by dissolving a flavonoid salt in an alcoholic or aqueous solution, followed by the addition of the metal salt also in alcoholic or aqueous solution. The reaction can be carried out under different conditions of stirring and/or heating, normally a base is used to deprotonate the hydroxyl groups and facilitate metal coordination. The complex usually precipitates from solution and is then filtered and air dried (**Table 1**). Preparations of ferrocenyl flavonoid complexes, where the ferrocenyl moiety acts as a replacement for ring B, follow a different synthetic approach. Ferrocenyl aurones are obtained via a classic Claisen-Schmidt condensation of ferrocene carboxaldehyde and various 2-hydroxyacetophenones to obtain the corresponding ferrocene chalcones [39, 40]. The synthesized chalcones are then treated with mercury acetate in pyridine to form the ferrocenyl aurones that can be isomerized into their flavone counterparts by heating in ethanol at reflux with potassium cyanide (**Figure 3**) [39, 40].

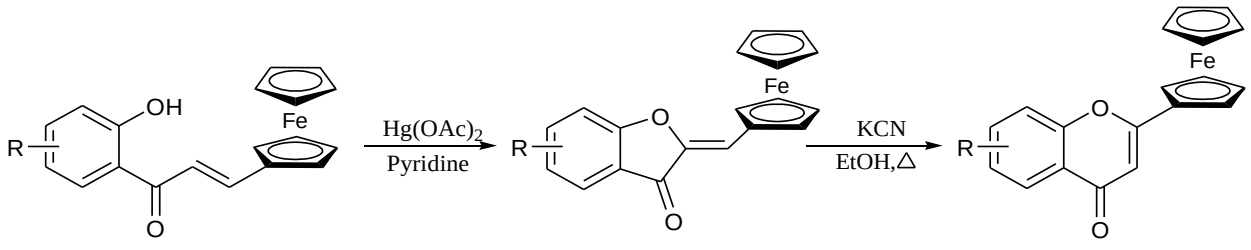

Ferrocenyl Chalcones Ferrocenyl Aurones Ferrocenyl Flavones

Figure 3. Synthesis of ferrocenyl flavonoids

Kowalski et al. reported the synthesis of ferrocenyl flavonoids using the palladium-catalyzed Heck cross-coupling reaction of vinyl ferrocene with 6-bromochromones (**Figure 4**) [41].

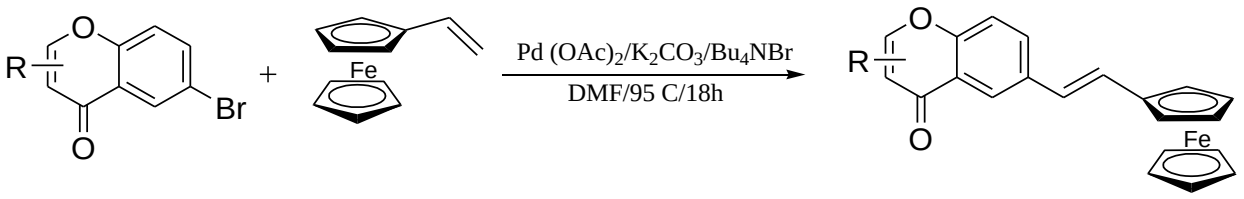

Figure 4. Synthesis of ferrocenyl flavonoids using Pd

Structural characterization of metal complexes can be achieved using a number of methods (**Table 1**). Fourier transform infra-red (FT-IR) spectroscopy can indicate the coordination site of the metal. Complexation of the metal atom with the C=O group, for instance, causes an increase in the bond length which is manifested as a decrease in the frequency of the C=O peak. Coordination with OH groups leads to disappearance of their characteristic broad peaks υ OH at 3600-3200 cm^{-1}. However, this disappearance can be masked by the presence of other OH groups in the flavonoid structure and in the H_2O molecules incorporated in the metal sphere during complexation. Therefore, IR spectroscopy is not a helpful tool in determining which OH groups are specifically coordinated to the metal atom. . ^{1}H NMR spectroscopic analysis can provide a better alternative where the disappearance of an OH peak from the ^{1}H NMR spectrum corresponds to coordination at this particular OH group. For example, the disappearance of the 5-OH peak at δ 10.52 ppm of the **lanthanum-18** complex proved coordination at this OH in ring A [42]. Heteroatom NMR spectroscopic analysis is also extremely useful. For example, Tabassum et al. used ^{119}Sn NMR spectroscopic analysis to prove the presence of stannous atoms in the synthesized bi-metallic complexes **31** and **32** (**Figure 6**) [43]. ^{195}Pt NMR spectroscopic analysis was also used to prove the structure of complex **68** [44]. Electron Paramagnetic Resonance (EPR) spectroscopy is also a helpful technique which is similar to NMR spectroscopy but more sensitive as it explores the interaction between an external magnetic field and unpaired electrons rather than nuclei. This is attributed to the fact that the amount of energy absorbed by a spinning electron is higher than that absorbed by a nucleus. This technique is more difficult to use as it requires background knowledge of subjects like quantum mechanics and mathematical techniques [45]. However it was used by Tabassum and Naso et al. groups to elucidate structures

of complexes (**31** and **32**) and (**33**, **37**, **VOhespiridin**, **VOsilibinin** and **VOmorin**), respectively [43, 46-49].

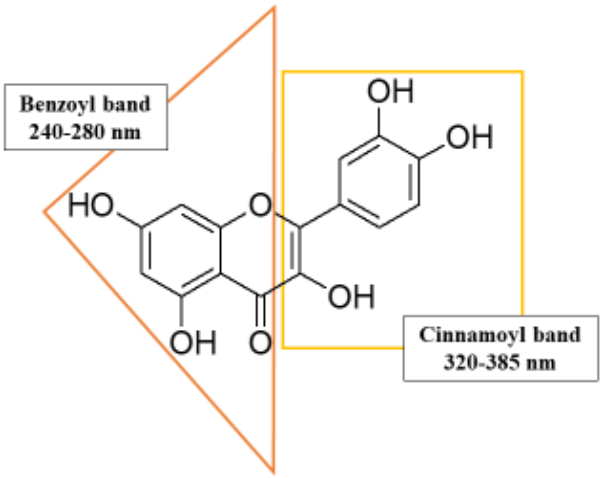

Figure 5. UV absorption bands using quercetin as an illustrative example

Flavonoids display absorption bands in the UV-Vis region due to electronic $\pi - \pi^*$ transitions [50, 51]. These transitions are responsible for the two characteristic benzoyl and cinnamoyl bands of flavonoids at 240-280 nm and 320-385 nm, respectively (**Figure 5**) which are bathochromically shifted after chelating with metals [52]. The observation of a red shift in one band rather than the other verifies chelation with that particular ring [53-55]. Although the shift is small in many cases, it gives a good insight when overlapped with the parent's spectrum. UV-Vis absorption bands are also characteristic to binding in other sites. Analysis of the spectra of **VOhespiridin** showed complexation with the rutinose sugar part [46]. Its electronic spectra showed bands at 358, 520 and 702 nm in agreement with the three band pattern at ca. 420, 500 and 700 nm observed for similar sugar vanadyl(IV) complexes coordinated through deprotonated cis-hydroxyl groups [56]. UV-Vis spectra can also help in detecting the stoichiometry of the complex. This is achieved by monitoring the absorption intensity of the ligand through a range of concentrations until the reaction is completed [46, 47, 57, 58]. Different methods can then be used to represent the data, e.g. Job's method, from which ligand-metal ratio can be interpreted. Similarly, fluorescence of free parents can be compared to their complexes at a specific wavelength. Peaks from complexes are higher in intensity and are shifted to lower wavelengths ca. 15-20 nm [55]. Elemental analysis and mass spectrometry provide complementary

information about the molecular formulae of the resulting complexes. In a recent study by Wang et al. the elemental analysis of a lead-luteolin complex was determined by scanning electron microscope (SEM) equipped with energy dispersive spectroscopy (EDS) [59]. The experimental values of weight and atomic number percentages of carbon, oxygen and lead atoms favored a 2:1 rather than 1:1 complex [59]. Analysis of the fragmentation pattern in mass spectrometry specifies how many metal atoms are coordinated in the complex [43, 60-64]. Roy et al. and Naso et al. reported the synthesis of two different complexes (**36** and **37** respectively) using the same ligand (**Luteolin**) and metal (**Vanadium**) [49, 65]. The two complexes are reported to differ in their stoichiometries and metal coordination sites which may have resulted from different ligand/metal ratios added during the synthesis process. Thus for complex **36**, two luteolin molecules are reported to chelate to the oxidovanadium(VI) group via the 4-C=O and 5-OH functionalities, whilst **37** is reported to contain only one luteolin chelated to the 3' and 4' cis-OH groups in ring B. Among the characterization techniques provided by Roy and his group, mass spectrometry data supported their structural hypothesis for complex **36**. Thus peaks at m/z 623.11, 639.89 and 658.21 represented two luteolin + one vanadium, two luteolin + vanadium oxide and two luteolin + vanadium oxide with one molecule of water, respectively. When deducing the structure of complex **37**, Nato et al. demonstrated that the FT-IR spectrum showed no change in the C=O and the C2=C3 bands, in addition to an increase of 44 cm^{-1} of the 4'-OH band, indicating chelation with ring B. EPR and UV-Vis spectra of complex **37** also supported the same findings. Thermal gravimetric studies provide information on the heat-induced decomposition of the complex as a function of temperature or time. Dehydration happens during the early stages at temperatures ranging from 100-250 ^{O}C. This is followed by decomposition of the ligand at higher temperatures (400-600 ^{O}C). At temperatures as high as 900 ^{O}C, the complex decomposes completely leaving the metal oxide [42, 43, 55, 60, 62, 66].

Nevertheless, the best proven technique to confirm a theoretical structure is X-ray crystallography. Unfortunately, it is not feasible to apply this to all synthesized molecules due to the specific crystal requirements needed to run an X-ray. Only structures of complexes **49**, **51**, **53** and **55** [67, 68] were proven by X-ray crystallography.

In general, all the used characterization methods can provide helpful information of varying importance. NMR and UV-Vis spectroscopy are the most insightful if X-ray is not feasible.

Other methods like IR spectroscopy, elemental analysis and mass spectrometry can complement the results obtained and offer the advantages of being easy to interpret and available in most research facilities.

168 **Table 1.** Summary of synthetic conditions and characterization methods for flavonoid metal complexes

Flavonoid Solution	*Metal*	*Base used and pH*	*Final product Formula*	*Characterization*	*Ref*
Quercetin.2H_2O in EtOH	$NiCl_2 \cdot 6H_2O$	NaOEt 6-7	$Ni(Que)_2(H_2O)_2$	UV IR Elemental Analysis	[54]
	$CuCl_2.2H_2O$	NaOEt 6-7	$Cu(Que)_2(H_2O)_2$	UV IR Elemental Analysis	[53]
	La acetate Nd acetate Eu acetate Gd acetate Tb acetate Dy acetate Tm acetate Y acetate	NaOEt *N.A.*	$La(Que)_3(H_2O)_6$ $Nd(Que)_3(H_2O)_6$ $Eu(Que)_{3(}H_2O)_6$ $Gd(Que)_3(H_2O)_6$ $Tb(Que)_3(H_2O)_6$ $Dy(Que)_3(H_2O)_6$ $Tm(Que)_3(H_2O)_6$ $Y(Que)_3(H_2O)_6$	UV IR ^1H NMR TG-DTA Fluorescence analysis Electrochemistry Elemental analysis	[55]

$[Cu(Que)_2(H_2O)_2]$ in MeOH	$SnCl_4$	*N.A.*	$[Cu(Que)_2(H_2O)_6\text{-}Sn_2Cl_4]$	IR ^{1}H, ^{13}C & ^{119}Sn NMR EPR ESI-MS TG-DTG	[43]
$[Zn(Que)_2(H_2O)_2]$ in MeOH	$SnCl_4$	*N.A.*	$[Zn(Que)_2(H_2O)_6\text{-}Sn_2Cl_4]$	IR ^{1}H, ^{13}C & ^{119}Sn NMR EPR ESI-MS TG-DTG	[43]
Chrysin in EtOH	Vanadyl acetylacetonate	*N.A.* 5	$VO(Chry)_2EtOH$	UV-Vis IR EPR Spectrophotometric titrations	[58]
	Ph_3GeBr	Na_2CO_3 *N.A.*	Chry-Ge. C_2H_6O	IR ^{1}H & ^{13}C NMR Elemental analysis	[69]

Luteolin in H_2O	La acetate	NaOH *N.A.*	$La(Chry)_2.OAc(H_2O)_7$	IR ^1H NMR Elemental analysis TG-DTG Spectrophotometric titrations	[57]
Luteolin	$VOSO_4.H_2O$	NaOH 6	$VO(Lut)_2$	UV-Vis IR ^1H NMR ESI-MS	[65]
Luteolin in EtOH	50% aqueous solution of $VOCl_2$	NaOH 5	$[VO(Lut)(H_2O)_2]Na\cdot 3H_2O$	UV-Vis IR EPR Elemental analysis	[49]
Hesperidin in H_2O	$Mn(CH_3COO)_2$	*N.A.* 4	MnO-Lut	UV-Vis IR Elemental analysis TG-DTG	[70]
	50% aqueous solution of $VOCl_2$	NaOH 12	$[VO(Hesp)(OH)_3].\ Na_4(H_2O)_3$	UV-Vis IR EPR Spectrophotometric	[46]

				titrations	
Hesperetin in EtOH	$CuCl_2.2H_2O$	NH_3 solution 7-8	$[Cu(Hespt)_2(H_2O)_2] \cdot H_2O$	UV-Vis IR ESI-MS TG-DTG	[66]
Naringin in MeOH	Cu acetate in distilled H_2O	*N.A.*	$[Cu\ (Nar)]^+[CH_3COO]^- \cdot (H_2O)_5$	UV-Vis IR ^1H NMR ESI-MS Elemental analysis	[71]
Naringenin in EtOH	$CuCl_2.2H_2O$	NH_3 solution 7-8	$[Cu(Narg)_2(H_2O)_2] \cdot H_2O$	UV-Vis IR ESI-MS TG-DTG	[66]
Apigenin in EtOH	$CuCl_2.2H_2O$	NH_3 solution 7-8	$[Cu(Apg)_2(H_2O)_2] \cdot H_2O$	UV-Vis IR ESI-MS TG-DTG	[66]
Silibinin in EtOH	50% aqueous solution of $VOCl_2$	$NaOCH_3$ 9	$Na_2[VO(Sil)_2].(H_2O)_6$	IR EPR Spectrophotometric titrations	[47]

Morin in MeOH	50% aqueous solution of $VOCl_2$	$NaOCH_3$ 5	$[VO(Mor)_2H_2O].(H_2O)_5$	UV-Vis IR EPR Spectrophotometric titrations	[48]
Kaempferol in EtOH	$ZnCl_2.2H_2O$	NaCl 8-10	$[Zn(Kaem)_2(H_2O)_2] \cdot H_2O$	UV-Vis IR ^1H NMR ESI-MS Elemental analysis	[64]
Niffcoumar sodium salt in H_2O	$Ce(NO_3)_3.6H_2O$ $La(NO_3)_3.6H_2O$ $Nd(NO_3)_3.6H_2O$	*N.A.* 4-5	$Ce(NS)_3.(H_2O)_4$ $La(NS)_3.(H_2O)_4$ $Nd(NS)_3.(H_2O)_6$	IR ^1H NMR Elemental analysis	[72]
Niffcoumar in H_2O	Aqueous solution of $ZrCl_4$	NaOH 5	$Zr(Niff)_2(OH)_4(H_2O)_5$	IR ^1H NMR Elemental analysis TG-DTG	[73]
Warfarin in H_2O	Aqueous solution of $ZrCl_4$	NaOH 5	$Zr(War)_2(OH)_4(H_2O)_2$	IR ^1H NMR Elemental analysis TG-DTG	[73]

Coumachlor in H_2O	Aqueous solution of $ZrCl_4$	NaOH 5	$Zr(Coum)_2(OH)_4(H_2O)_6$	IR ^1H NMR Elemental analysis TG-DTG	[73]
1 in 50% EtOH	GeO_2 in deionized H_2O	NaOH 7	*N.A.*	UV-Vis IR ^1H NMR MS Elemental analysis TG-DTG	[62]
2-11 in MeOH	[Ru(η6-p-cymene)Cl_2]$_2$ in CH_2Cl_2	NaOMe *N.A.*	*N.A.*	^1H & ^{13}C NMR Elemental analysis X-ray for (49, 51, 53, 55)	[67, 68]
15-18 in CH_2Cl_2	[Ru(η6-p-cymene)Cl_2]$_2$ in CH_2Cl_2	*N.A.*	*N.A.*	UV-Vis spectra IR ^1H NMR FAB/EI-MS	[61, 68, 74]
7, 12-14 in EtOH	$[Ru(DMSO)_4Cl_2]$ in EtOH	TEA *N.A.*	$[Ru(DMSO)_2(7)_2]_2NaNO_3(H_2O)_2$ $[Ru(DMSO)_2(12)_2]_2NaNO_3.\ H_2O$ $[Ru(DMSO)_2(13)_2].\ (NO_3)_2(H_2O)_2$ $[Ru(DMSO)_2(14)_2]_2NaNO_3(H_2O)_5$	IR ^1H NMR ESI-MS Elemental analysis	[63]

18 in EtOH	$La(NO_3)_3.6H_2O$	TEA *N.A.*	*N.A.*	UV-Vis spectra IR ^1H NMR Elemental analysis TG-DAT	[42]
19 in H_2O	Aqueous solution of Ce La Nd	NaOH 5	$Ce(19)(OH)(H_2O)_2$ $La(19)(OH).H_2O$ $Nd(19)(OH).H_2O$	IR ^1H & ^{13}C NMR Elemental analysis	[75]
20 in EtOH	Aqueous solution of K_2PtCl_4	*N.A.*	cis - $[Pt(20)_2Cl_2]$	IR ^1H & ^{195}Pt NMR	[44]

N.A.: Not available

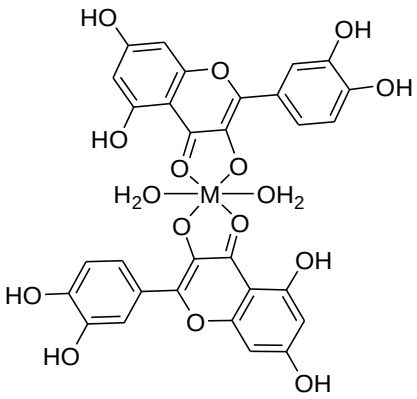

21, M = Ni; 22, M = Cu

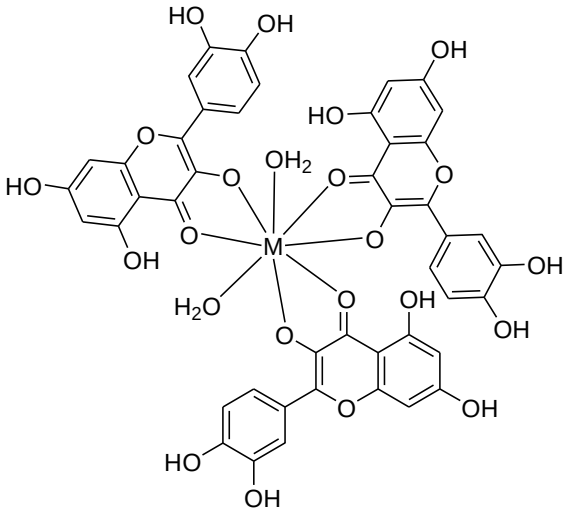

23, M = La; 24, M = Nd; 25, M = Eu; 26, M = Gd; 27, M = Tb; 28, M = Dy; 29; M = Tm; 30, M = Y

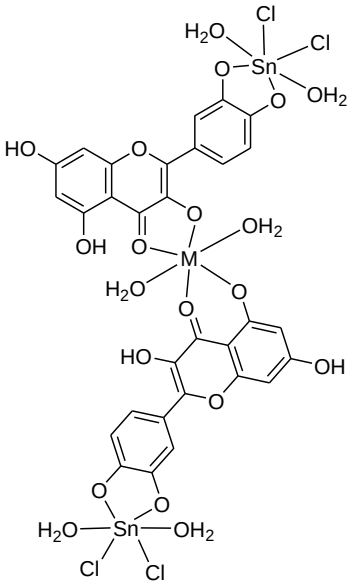

31, M = Cu; 32, M = Zn

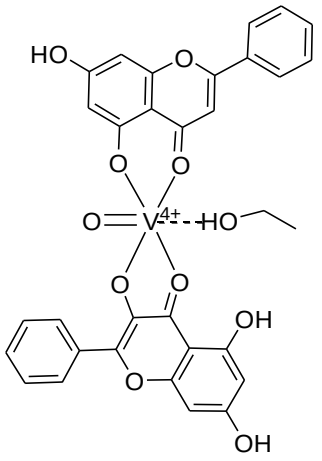

33

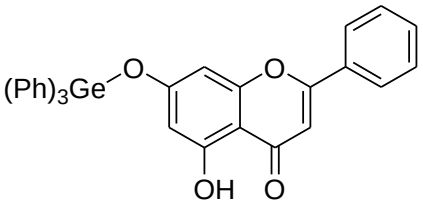

34

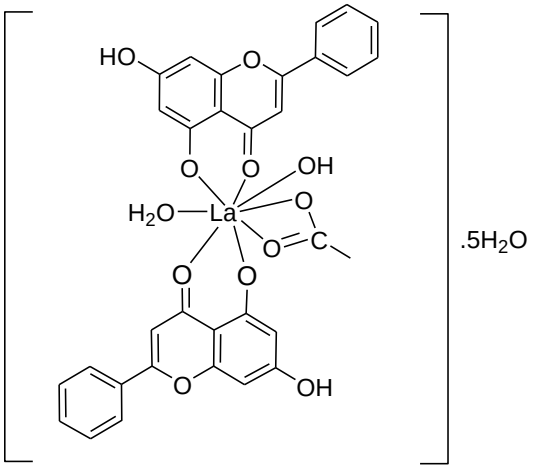

35

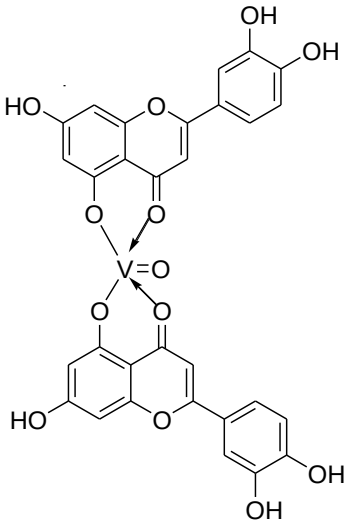

36

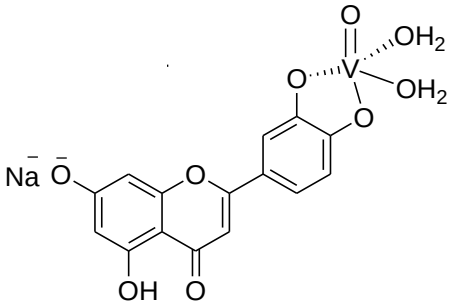

37

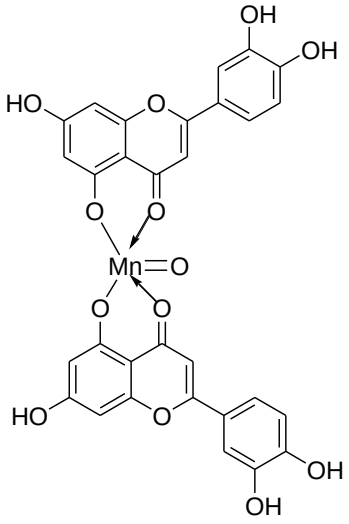

38

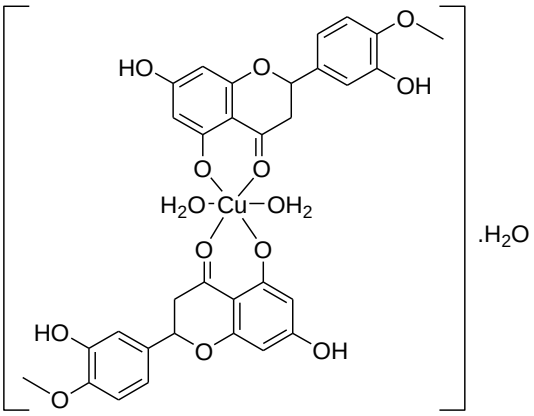

39

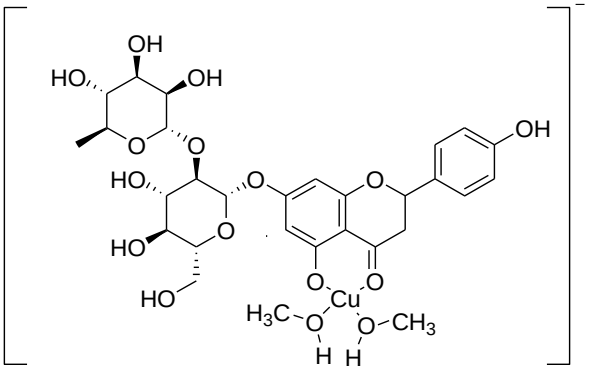

40

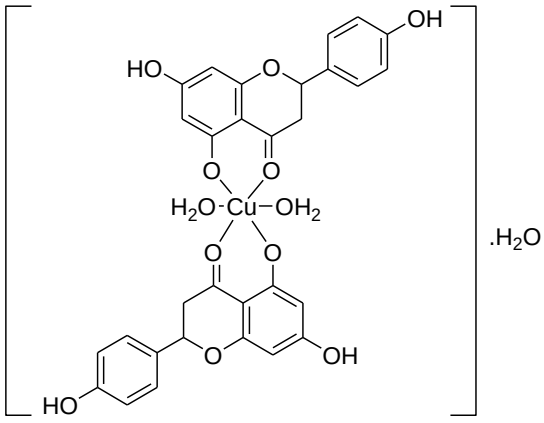

41

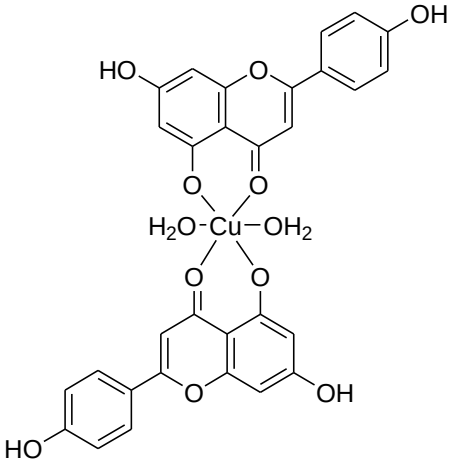

42

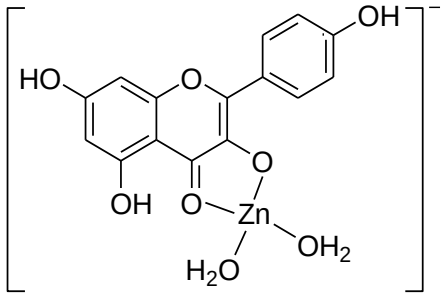

43

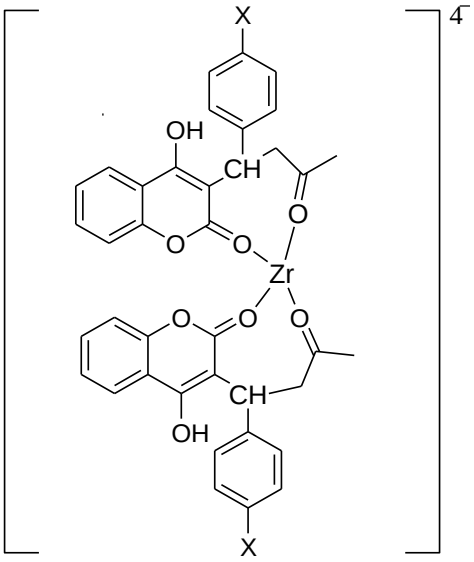

44, X = NO_2; 45, X = H; 46, X = Cl

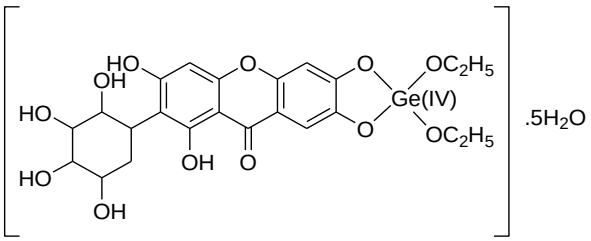

47

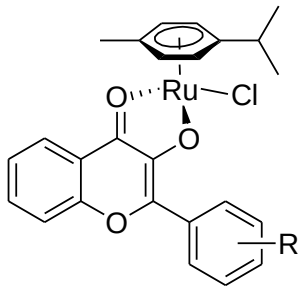

48, R = H; 49, R = *p*-CH_3; 50, R = *p*-F; 51, R = *m*-F; 52, R = *o*-F; 53, R = *p*-Cl; 54, R = *m*-Cl; 55, R = *o*-Cl; 56, R = *p*-Br; 57, R = *m*-Br; 58, R = *p*-OCH_3; 59, R = *p*-NO_2; 60, R = *p*-NMe_2

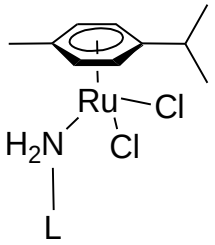

61, L = Cpd 15; 62, L = Cpd 16; 63, L = Cpd 17

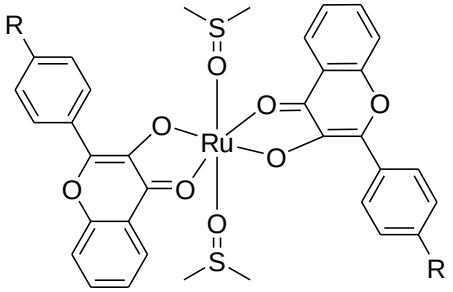

64, R = Cl; 65, R = OCH_3; 66, R = NO_2; 67, R = NMe_2

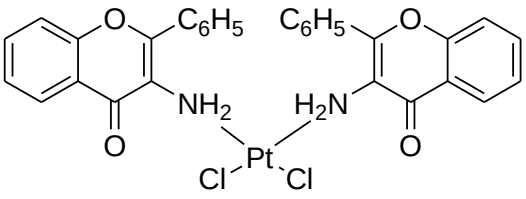

68

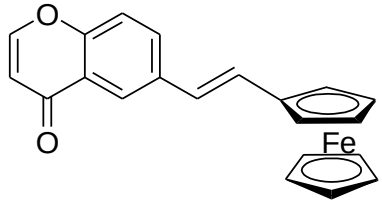

69

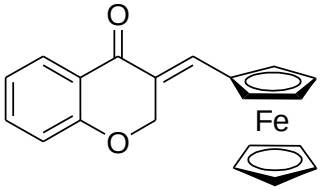

70

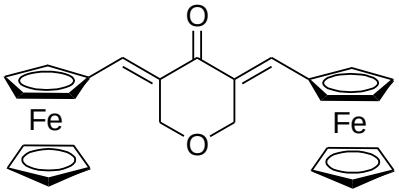

71

175

176 **Figure 6.** Chemical structures of flavonoid metal complexes

Anti-oxidant activities of flavonoid metal complexes

Complexation of flavonoids with metals often increases the anti-oxidant activity of the parent flavonoids as shown in table 2. Metal complexes demonstrate enhanced activities in free radical scavenging assays such as $DPPH^{\cdot}$ (1,1-diphenyl-2-picrylhydrazyl radical), $ABTS^{+}$ [2,20-azino-bis(3-ethylbenzothiazoline-6-sulfonic acid diammonium salt)], H_2O_2, $OH^{\cdot}$ and $O_2^{-\cdot}$. Superoxide dismutase (SOD) like activity is often used to measure the anti-oxidant activities of the complexes as it is considered to be one of the body's first line free radical defense enzymes.

However, it is important to note that even where the complexes showed better SOD like activity than their free parents they are still far above the limit for good SOD like activity which is $IC_{50} \leq 20$ µM.

Table 2. Summary of anti-oxidant activities of reviewed flavonoids and their metal complexes

Complex	Assay	Results	Ref
23 **24** **25** **26** **27** **28** **29** **30**	$O_2^{-\cdot}$	Enhanced activity at 120 µM, 90% 85% 84% 97% 77% 92% 87% 88% ***quercetin = 42%***	[55]
33	$DPPH^{\cdot}$	Enhanced activity at 100 µM, 45% ***chrysin = 18%***	[58, 76]
	$ABTS^{+}$	Enhanced activity 3.96 mM ***chrysin = 0.9 mM***	

	SOD	IC_{50} = 157 µM ***chrysin = no activity***	
	$OH^{\cdot}$	Enhanced activity at 100 µM, 75% ***chrysin = 45%***	
36	$DPPH^{\cdot}$	Enhanced activity at 100 µM, 40% ***luteolin = 25%***	[65]
	$ABTS^{+}$	Enhanced activity at 10 µM, 64% ***luteolin = 40%***	
37	$DPPH^{\cdot}$	Lower activity IC_{50} = >100 µM ***luteolin = 66.7 µM***	[49]
	$OH^{\cdot}$	Enhanced activity IC_{50} = 17 µM ***luteolin = 50.7 µM***	
	$O_2^{-\cdot}$	Lower activity IC_{50} = 417 µM ***luteolin = 384 µM***	
38	$DPPH^{\cdot}$	Enhanced activity at 1 mM, 90% ***luteolin = 75%***	[70]
	$OH^{\cdot}$	Enhanced activity at 1 mM, 80% ***luteolin = 74%***	
VOhesperidin	$DPPH^{\cdot}$ $ABTS^{+}$	No enhancement in activity	[46]
40	$DPPH^{\cdot}$	Enhanced activity at 10 µM, 35.5% ***naringin = 2%***	[71]

VOmorin	SOD	Slightly enhanced activity IC_{50} = 45 µM ***morin = 66 µM***	[48]
	$DPPH^{\cdot}$	Similar activity at 10 µM, 22% ***morin = 15%***	
	$ABTS^{+}$	Similar activity at 10 µM, 81% ***morin = 76%***	
	$OH^{\cdot}$	Enhanced activity at 10 µM, 26% ***morin = 2%***	
	$ROO^{\cdot}$	No effect on radical	
47	$OH^{\cdot}$	Enhanced activity at 100 µM, 65% ***2 = 43%***	[62]
	$DPPH^{\cdot}$	Lower activity at 80 µM, 60% ***2 = 95%***	

As shown in table 2, rare earth metal complexes (**23-30**) increased $O_2^{-\cdot}$ scavenging activity of quercetin by, on average, 2-fold [55]. The difference in activity between the eight metal complexes is not significant, however, the gadolinium complex (**26**) showed the best activity. Whether this increase in activity is attributed to incorporation of the metal atom or to the higher molar ratio of quercetin present in the complex (as opposed to 1 quercetin molecule) needs further investigation. **Figure 7** illustrates the main structural features responsible for the anti-oxidant activity of flavonoids. The 3', 4' *ortho*-dihydroxyl group is the most significant contributor to flavonoids' anti-oxidant activity [3]. These two catechol moieties form *ortho*-semiquinone radicals that are highly stabilized by the electron delocalization and intra-molecular hydrogen bonding. The combination of C2=C3 and 4-C=O group in ring C also assists in the

delocalization of the π-electrons in ring B. This in turn influences the dissociation of phenolic hydroxyl groups as well as the stability of the formed phenoxy radicals in ring B [3]. Ring A *meta*-hydroxyl groups are less important than ring B dihydroxyl groups which are oxidized more readily [77]. The highest increase in activity can be seen upon complexation of metals with flavonoids lacking the essential structural features of anti-oxidant activity (**Figure 7**), such as chrysin and naringin [78]. For instance, complexation of vanadium metal with chrysin (**33**) increased $ABTS^{\cdot+}$ scavenging activity from 0.9 mM for chrysin to 3.96 mM [58]. This value is close to that of quercetin (4.7 mM) [79] that fulfills anti-oxidant structural activity requirements (**Figure 7**) and is therefore one of the best flavonoid anti-oxidants.

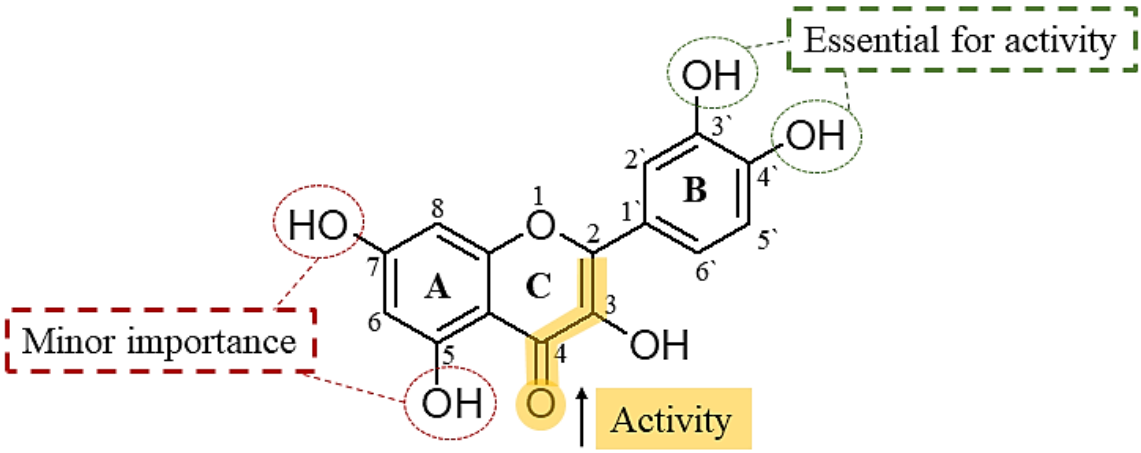

Figure 7. Summary of structural features responsible for anti-oxidant activity of flavonoids

As illustrated in **Figure 8**, metal complexation demonstrated a positive impact on the $DPPH^{\cdot}$ scavenging activity of ligands which was higher than that of vitamin C in only one case, the Cu-Naringin complex **40**. Despite the witnessed increase in $DPPH^{\cdot}$ scavenging activity of chrysin (18%) upon complexation with vanadium (**33**) (45%) at 100 µM, it is still far less than that of ascorbic acid (98%) at the same concentration [58]. However, metal complexation did not always result in enhanced $DPPH^{\cdot}$ scavenging activity. The vanadium-luteolin complex **37** showed a loss in the $DPPH^{\cdot}$ scavenging activity of luteolin due to chelation of the vanadium metal with the 3' and 4'-OH groups that are essential for anti-oxidant activity of flavonoids [49]. Pi et al. attributed the loss of the polyphenol ligand's (**2**) high $DPPH^{\cdot}$ scavenging activity (95%)

after coordination with germanium (**47**) to steric hindrance factors [62]. This might be caused by the presence of the two ethyl ether groups rather than the germanium atom.

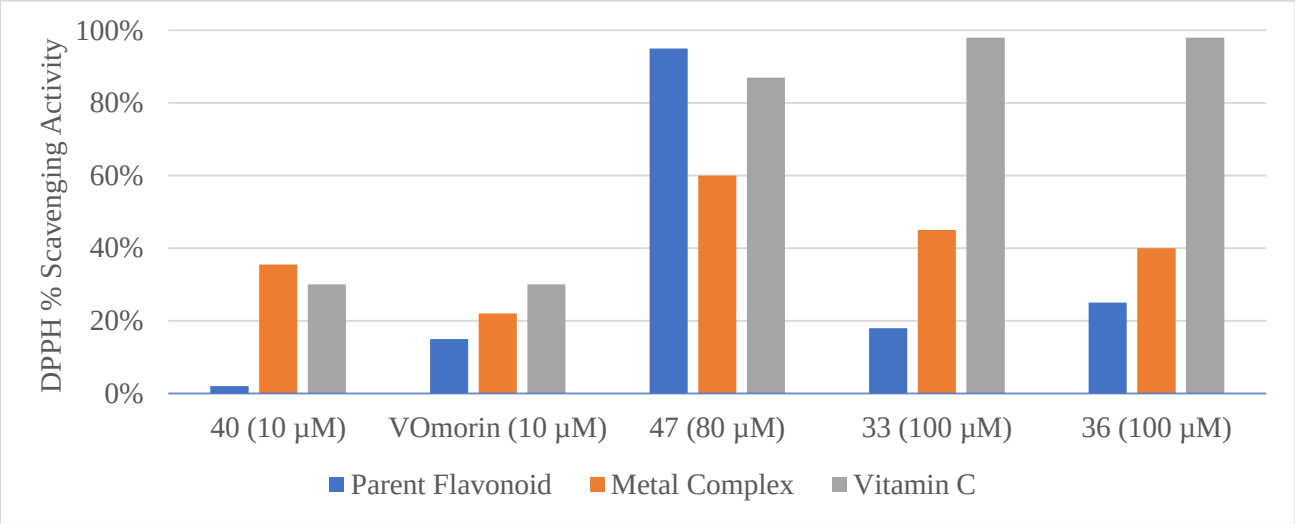

Figure 8. DPPH· scavenging activity of metal complexes compared to their parent flavonoids and vitamin C at different concentrations

Cytotoxic activities of flavonoid metal complexes

One of the milestones in the history of chemotherapy was the discovery of cisplatin in 1969 [80]. Cisplatin is effective and still widely used against various types of cancers, such as testicular, ovarian, breast, bladder, lung cancer and brain tumors. It demonstrates remarkable curing rates for testicular cancer (over 90% and near 100% with early discovery) [81]. Inside the body, cisplatin crosslinks DNA and initiates apoptosis. Despite this promising profile, cisplatin suffers from limitations such as nephrotoxicity, neurotoxicity and drug resistance [82, 83]. This ongoing interest in the design and development of metal-based anti-cancer drugs has also influenced the flavonoid field, where a number of flavonoid-metal complexes have been synthesized and evaluated as anti-cancer agents.

Cytotoxic activity of quercetin metal complexes

Table 3. Summary of *in vitro* anti-tumor activity of quercetin metal complexes

Complex	Cell line	Activity (μM) (IC_{50} or suppression % or GI_{50})	Quercetin activity (μM)	Ref.
21	HepG2	14.4 ± 0.9 *	33.7 ± 1.0 *	[84]
	SMMC7721	19.6 ± 0.6 *	42.1 ± 1.0 *	
	A549	35.6 ± 0.8 *	72.1 ± 1.2 *	
22	A549	21.5 ± 0.5 *	34.9 ± 1.0 *	[53]
23	Bel-7402	46.03% ♦	20% ♦	[55]
25	Bel-7402	62.32% ♦	20% ♦	
26	Bel-7402	45.30% ♦	20% ♦	
31	U373MG, PC3, Hop62, HL60, HCT15 and HeLa	< 8.7 •	*N.A.*	[43]
32	HeLa	7.7 •	*N.A.*	

* = IC_{50}, ♦ = Suppression % at 10 μM, • = GI_{50}

Hepatocellular carcinoma (HepG2), hepatoma (SMMC7721), lung carcinoma (A549), liver cancer (Bel-7402), central nervous system (U373MG), prostate cancer (PC3), lung cancer (Hop62), leukemia (HL60), colon carcinoma (HCT15) and cervical cancer (HeLa).

It is evident that complexation with metals enhances the anti-proliferative activity of quercetin. Compound **21** (Ni-quercetin) had better activity on the hepatic cancer cell lines (HepG2 and SMMC7721) than on the lung carcinoma cell line (A549). Pro-apoptotic ability has been investigated for complexes **21** and **22** (Cu-quercetin) as a possible cytotoxic mechanism (**Figure 9**) [53, 84]. This is indicated by changes in the levels of key apoptotic proteins like survivin and caspases along with morphological changes observed using the DNA-sensitive Hoechst33258 stain. Possible mechanisms of action of **21** on the A549 cell line were not evaluated. This might have given a better idea of the behavior of complexes in different cell lines and the reasons behind the witnessed difference in activities.

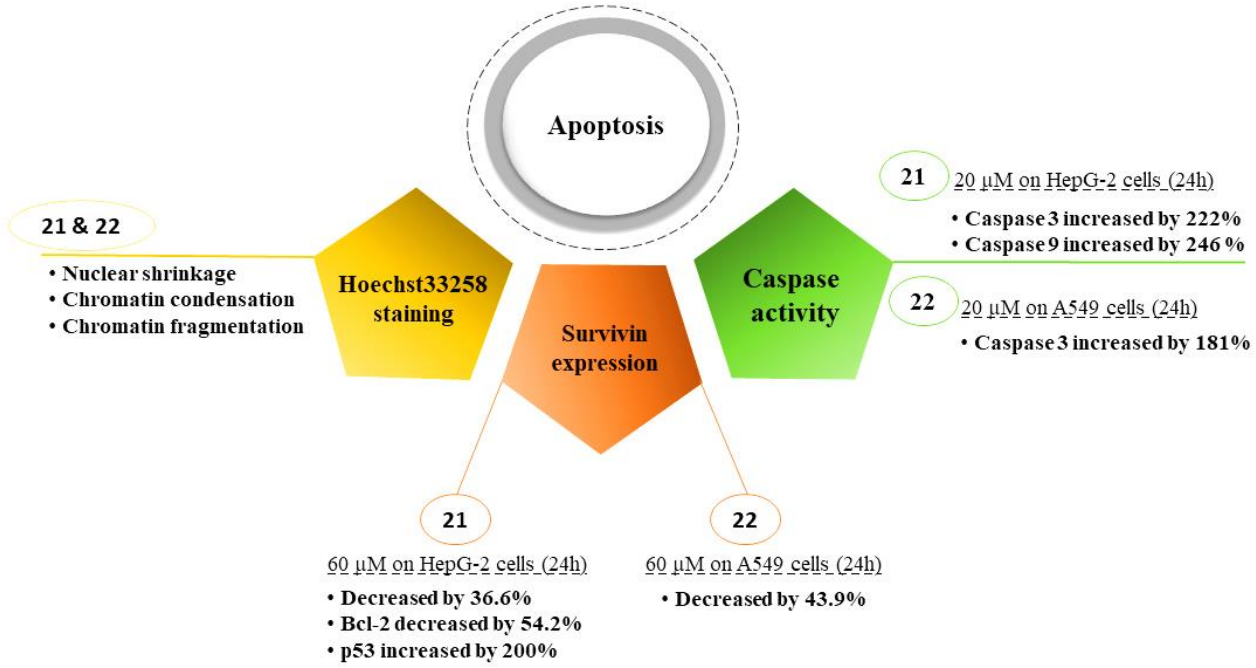

Figure 9. Summary of pro-apoptotic studies done on complexes 21 and 22. Survivin expression was measured by immunocytometry and caspase activity by absorption spectra.

Metal atoms in flavonoid complexes can interact with DNA nucleotides by either electrostatic interactions with the phosphate groups, or covalent binding to nucleobases (**Figure 10**). The ROS and free radicals resulting from flavonoids' auto-oxidation are thus generated in proximity to the DNA [37]. This leads to oxidative damage of DNA and induces apoptosis (**Figure 10**) [85, 86]. Flavonoid metal complexes are also more planar than the free ligands which facilitates their binding to DNA via intercalation [37]. Tan et al. reported the selective binding of the nickel quercetin complex (**21**) to GC-rich DNA sequences using fluorescence emission and molecular modelling. This, in addition to decreased survivin activity, led them to conclude that down regulation of survivin via interference with the GC-rich survivin protein promoter gene might be a plausible mechanism by which the complex **21** exerts its anti-tumor activity [84].

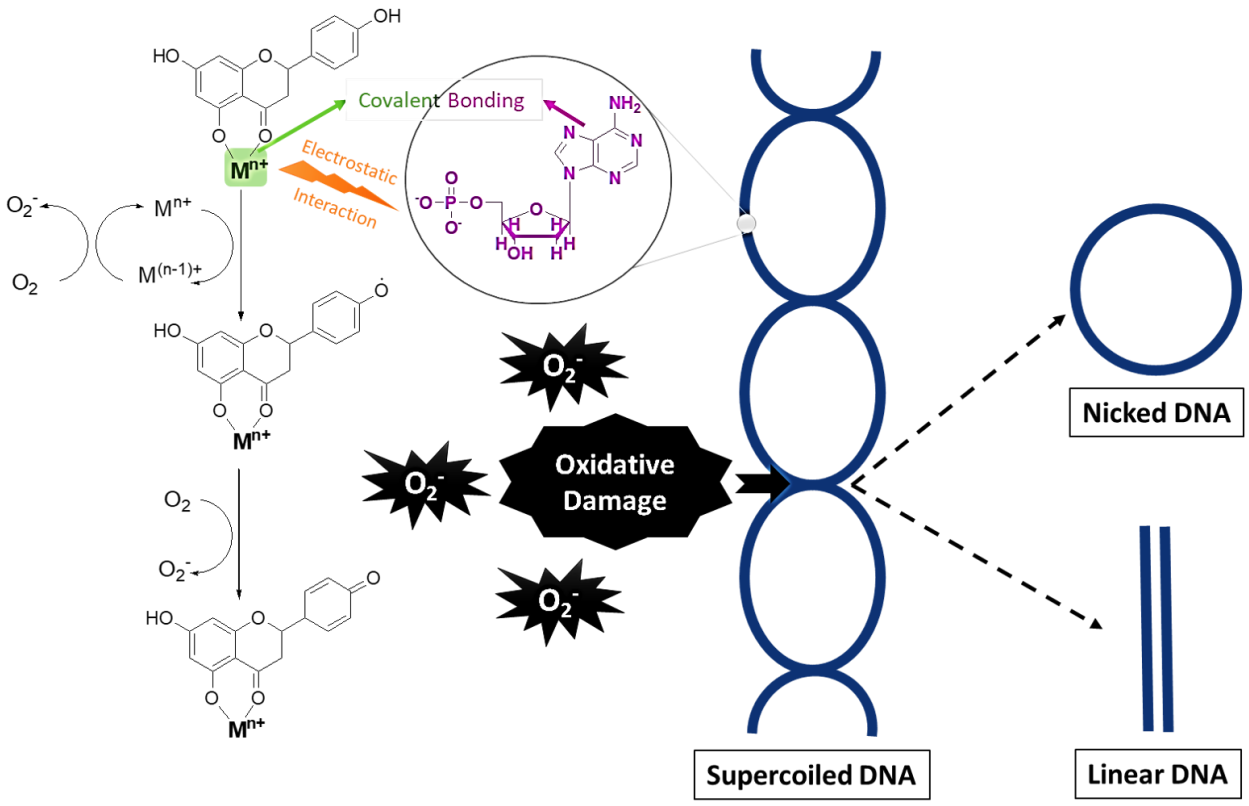

Figure 10. Plausible mechanism of oxidative DNA damage by flavonoid metal complexes

The quercetin rare earth metal complexes (**23**, **25** and **26**) showed increased activities compared with free quercetin on the liver cancer cell line (Bel-7402) (**Table 3**) [55]. Complex **23** (La-quercetin) can intercalate with DNA as evidenced by DNA fluorescence studies. Tabassum and her colleagues were able to synthesize two unique hetero-bimetallic complexes quercetin–Cu^{II}–Sn_2^{IV} (**31**) and quercetin–Zn^{II}–Sn_2^{IV} (**32**) [43]. The Cu complex (**31**) showed significant activity on various human cancer cell lines (**Table 3**) except for ovarian cancer (A2780). The Zn complex (**32**), however, did not demonstrate good activity except on the HeLa cell line (**Table 3**). Complexes **22**, **31** and **32** were able to promote the conversion of substrate DNA to cleaved forms (nicked and linear) as studied by gel electrophoresis [43, 53, 54]. To better understand whether this DNA cleavage is promoted through an oxidative pathway, the effect of different radical scavengers was evaluated where only H_2O_2 markedly promoted plasmid DNA breakage caused by the complexes. Increased level of thiobarbituric acid reactive species (TBARS) with increasing concentrations of complex **22** backs up the role of oxidative damage as a mechanism of CT-DNA cleavage [53, 54]. At 30 µM of complex **31**, DNA relaxation activity of

Topoisomerase-I was significantly inhibited. This does not necessarily correlate with direct inhibition of the enzyme and may instead result from strong binding with DNA which prevents the enzyme from exercising its function [43]. To exploit binding of complexes **31** and **32** with the minor groove of DNA, the complexes were docked into the DNA duplex of sequence d(CGCGAATTCGCG)2 dodecamer (PDB ID: 1BNA). Both complexes bound to the narrow minor groove region of DNA within the GC rich region and were stabilized by hydrogen bonding (2.8–3.0 Å) between the –OH groups of quercetin with O4/N2 atoms of C8/G8 bases in DNA.

Complex **31** also showed good binding modes with the human-DNA–Topo-I complex (PDB ID: 1SC7) and bovine erythrocyte Cu, Zn superoxide dismutase (PDB ID: 2SOD) [43].

Cytotoxic activity of chrysin, luteolin and silibinin metal complexes

Table 4. Summary of *in vitro* anti-tumor activity of metal complexes of chrysin, luteolin and silibinin

Complex	Cell line	Activity (μM) (IC_{50} or suppression %)	Flavonoid activity (μM)	Ref.
33	MG-63	16 *	>100 *	[76]
	HT-29	45% ◊	No effect ◊	[87]
VOsilibinin	HT-29	45% ◊	No effect ◊	
34	HepG2	30% ♦	20% ♦	[69]
	Colo205	25% ♦	10% ♦	
	MCF-7	45% ♦	20% ♦	
	MCF-7 10A	15% ♦	10% ♦	
35	A549	73.5 % ♦	4.9 % ♦	[57]
37	A549	60.5 *	66.3 *	[49]
	MDAMB-231	17 *	88.3 *	

* = IC_{50}, ♦ = Suppression % at 10 μM, ◊ = Suppression % at 100 μM
Osteosarcoma (MG-63), colon adenocarcinoma (HT-29), hepatocellular carcinoma (HepG2), caucasian colon adenocarcinoma (Colo205), breast cancer (MCF-7), breast cell line (MCF-7 10A), lung carcinoma (A549) and triple negative breast cancer (MDAMB-231).

The vanadium chrysin complex (**33**) showed significant cytotoxic activity on a human osteosarcoma cell line (MG-63) with an IC_{50} value of 16 µM (**Table 4**) [76]. This activity is higher than the reported activity of cisplatin on the same cell line (IC_{50} = 28.5 µM), yet lower than that of doxorubicin (IC_{50} = 3.35 µM) [88]. According to Leon et al. complex **33** showed a multi-factorial anti-tumor mechanism of action. For example, it demonstrated cytotoxicity to lysosomes and mitochondria of MG-63 cell line (at concentrations from 2.5 to 25 µM) as evidenced using neutral red (NR) uptake and the reduction of 3-(4,5-dimethylthiazol-2-yl)-2,5-diphenyltetrazolium bromide (MTT) assays, respectively. Genotoxicity was also evident through induced micronuclei formation and DNA breaks using the Comet assay, in the concentration range 2.5-5 µM. In addition to that, compound **33** lowered GSH/GSSG ratio in MG-63 cell line especially at higher doses (40%, 50 and 100 µM). In a protein array platform test, **33** upregulated 82 proteins and downregulated 9 such as PKB/AKT, Cdk 4, 6 and 7, NAK, and JNK [89]. It induced apoptosis via:

- Externalization of the phosphatidyl serine (PS), at the outer plasma membrane leaflet measured by Annexin V-FITC fluorescent probe.
- Alteration of the mitochondria membrane potential (MMP) measured by Rhodamine 123 that leads to the release of cytochrome c and finally to DNA fragmentation.
- Activation of caspase pathway measured by caspase 3 activation (350% basal at 100 µM).

In another report the anti-tumor activities of vanadium complexes of chrysin (**33**) and silibinin (**VOsil**) were tested on the HT-29 cell line (**Table 4**) [87]. **33** and **VOsil** showed better anti-proliferative activities than cisplatin at 100 µM (inhibition rate = 12 %) on the same cell line. However, **33** did not show pro-apoptotic effects in the MG-63 cell line despite it causing cell cycle arrest in the G2/M phase after 24 and 48 hours incubation. **VOsil**, on the other hand, increased the percentages of apoptotic/necrotic cells, induced caspase 3 activation and reduced nuclear factor kappa-light-chain-enhancer of activated B cells (NF-κB) that controls DNA transcription and is aberrantly activated in many cancers. Moreover, **VOsil** fully inhibited topoisomerase-IB using plasmid relaxation assay at 100 µM. The germanium complex of chrysin, (**34**) also had activity on several targets. Its cytotoxic effect on HepG2, Colo250 and MCF-7 cell lines was not significantly high nor much better than chrysin [69, 90]. The mean apoptotic population detected on MCF-7 and Colo205 cell lines by Annexin-V were 19.5% and

12.5% for 20 µg/ml, respectively. Additionally, cellular ROS production increased in MCF-7 cell line upon addition of high doses of complex **34**. This could be a possible etiology for apoptosis alongside with caspase-3, 8 and 9 activation whose levels increased from 100% to 214.5%, 181.1% and 286.0%, respectively at 20 µg/ml. Some caspase activation was also observed on the Colo205 cell line with an increase from 100% to 129.3%, 146.5 and 119.3%, for caspase-3, 8 and 9, respectively. Cell cycle arrest at the G2/M phase was detected on MCF-7 and Colo205 (high doses) cell lines and at the S phase with low doses of the complex on the Colo205 cell line. Complex **35** (La-chrysin) showed a significant increase (73.5%) in the anti-proliferative activity of chrysin (4.9%) on A549 cell lines. The complex intercalated with DNA base pairs as illustrated by an increase in viscosity and fluorescence of DNA upon addition of complex **35** [57]. The vanadium luteolin complex (**37**) significantly improved the cytotoxic activity of its parent on the MDAMB-231 cell line (IC_{50} = 17 µM) as shown in table 4 [49]. However, it showed a trivial improvement on the A549 cell line (IC_{50} = 60.5 µM, luteolin IC_{50} = 66.3 µM). Naso et al. carried out high content cytotoxicity assays on complex **37** to investigate its mechanism of action on the MDAMB-231 cell line. The tests included ROS production, MMP, plasmatic membrane damage, nuclear membrane damage and mitotic arrest. Complex **37** showed significant increase in the levels of ROS production (650%) and percentage of depolarized cells (20%). Lactate dehydrogenase (LDH) levels in the culture media were measured as an indication for plasmatic membrane damage. Complex **37** demonstrated 212% increase compared with the basal levels as opposed to 98% for luteolin. The vanadium complex (**37**) also showed DNA damage and mitotic arrest activities using H2AX and PHH3 assays, respectively.

Cytotoxic activity of hesperidin, naringin, hesperitin, naringenin, apigenin, morin, kaempferol, warfarin and mendiaxon metal complexes

Table 5. Summary of *in vitro* anti-tumor activity of hesperidin, naringin, hesperitin, naringenin, apigenin, morin, kaempferol, warfarin and mendiaxon metal complexes.

Complex	Cell line	Activity (suppression %)	Flavonoid Activity	Ref.
VOhesperidin	Caco-2	60% (at 100 µM)	No effect	[46]
40	K562	38.4% (at 100 µM)	13.2% (at 100 µM)	[71]
La-18	HL60	50% (at 0.01 µM)	*N.A.*	[42]
	A549	100% (at 0.003 µM)	*N.A.*	

39	HeLa	22.5%	15%	[66]
	SGC-7901	45%	30%	
	HepG2	45%	30%	
41	HeLa	24%	27%	
	SGC-7901	25%	33%	
	HepG2	35%	15%	
42	HeLa	25%	10%	
	SGC-7901	45%	5%	
	HepG2	35%	5%	
VOmorin	T47D	43% (at 10 µM)	No effect	[48]
	SKBR3	38% (at 10 µM)	14% (at 10 µM)	
43	EC9706	72% (at 30 µg/ml)	45 % (at 30 µg/ml)	[64]
45	HL60	30% (at 100 µM)	*N.A.*	[73]

Colon adenocarcinoma (Caco-2), chronic myeloid leukemia (K562), leukemia (HL60), lung carcinoma (A549), cervical carcinoma (HeLa), gastric carcinomas (SGC-7901) and hepatocellular carcinoma (HepG2), breast cancer (T47D), breast cancer overexpressing Herceptin-2 (SKBR3) and oesophageal cancer cell line (EC9706).

As shown in table 5, **VOhesperidin** showed 60% inhibition in cellular proliferation of the colon adenocarcinoma cell line (Caco-2) while its parent hesperidin showed no effect at all on the same cell line at 100 µM [46]. The Cu naringin complex (**40**) exhibited better inhibition of the K562 cell lines (**Table 5**). Cell cycle analysis showed a 50% decrease in viable cells at the S/G2/M phases after 24 h. The number of hypodiploid cells tremendously increased from 5.5% (control) to 38.4% indicating the complex led to cell death in the first 24 h [71]. The lanthanum complex with ligand **18** exhibited a stronger suppression rate (100% inhibition at 0.003 µM) than cisplatin (100 % inhibition at 0.004 µM) on the A549 cell line [42]. Lanthanum complexes like **35** and **La-18** have significantly high suppression rates on A549 cell line.

As shown in table 5, complexation of copper with the flavonoids hesperetin (**39**) and apigenin (**42**) did enhance the anti-proliferative activity of their free flavonoids whilst the naringenin complex (**41**) did not show any improvement except on the HepG2 cell line [66]. **41** and **42** had the same suppression rate (35%) on the HepG2 cell line. This indicates that unsaturation of ring C has no effect on the activity whilst the addition of an OH group on ring B, as in complex **39**, results in 30% increase in the activity. This may be due to the enhanced anti-oxidant activity of

compounds featuring two *m*-hydroxyl groups on ring B (**Figure 7**). Several DNA binding studies (UV-Vis spectral, fluorescence and CD measurements) were performed with the complex **39** that indicated DNA binding via intercalation with higher affinity than the free ligand.

The vanadium morin complex (**VOmor**) showed promising cytotoxic activity on human breast cancer cell lines (**Table 5**). It did not have deleterious effects on the non-tumorigenic breast epithelial mammal cells indicating its selectivity towards cancer cells [48]. Naso et al. suggest that the **VOmor** complex causes cell death by induction of apoptosis. This can be correlated to perturbation of the mitochondrial membrane potential which results in release of cytochrome c from the mitochondria to cytosol. This process leads to the activation of caspases-9, 3 and 7. However, mitochondrial membrane potential was only observed in the SKBR3 cell line which suggests the apoptotic potential on the T47D is achieved via a different mechanism that needs further investigation. The MTT assay was used to determine the anti-proliferative activity of the Kaempferol Zn complex (**43**) on EC9706 cells (**Table 5**) [64]. Cell viability decreased nearly by half in the EC9706 cell line while no significant effect was observed on the normal kidney cells (HK-2 cells). Atomic force microscopy (AFM) morphological data showed that complex **43** could deform and shrink EC9706 cells at the nanoscale. To measure apoptosis induction ability, Annexin V-FITC/PI was used. The apoptosis ratio of EC9706 cells increased from 3.4 ± 0.9% for control cells to 33 ± 7.6% upon raise of **43** concentrations from 0 to 30 μg/mL, respectively. Complex **43** was able to increase the intracellular calcium ion level in cancer cells that can mediate cell death.

Cytotoxic activity of metal complexes 47-71

Table 6. Summary of *in vitro* anti-tumor activity of complexes **47-71**

Complex	Cell line	Activity (μM) (IC_{50} or suppression%)	Flavonoid activity (μM)	Ref.
47	HepG2	65% ♦	35% ♦	
51	CH1	1.5 *	*N.A.*	[67, 68]
53		0.86 *	0.6 *	
54		1 *	*N.A.*	
55		1.2 *	*N.A.*	
61	DMBC12	0.96 *	*N.A.*	[61]

62	DMBC11	1.13 *	*N.A.*	[63]
63		2.53 *	*N.A.*	
		4.14 *	*N.A.*	
64	MCF-7	16 *	17.2 *	
65		28 *	29.5 *	
66		32.1 *	35.4 *	
67		36.2 *	38.4 *	
Ce-19	HL60	21.37 *	*N.A.*	[75]
69	CCRF-CEM	37.5 *	*N.A.*	[41]
70	Jurkat	2.97 *	*N.A.*	[91]
	HeLa	7.23 *	*N.A.*	
71		7.4 *	*N.A.*	

* = IC_{50}, ♦ = Suppression % at 160 µM

Hepatocellular carcinoma (HepG2), ovarian cancer (CH1), patient derived (not-established) melanoma (DMBC11 and DMBC12), breast cancer (MCF-7), lung carcinoma (A549), cervical carcinoma (HeLa), chronic myelogenous leukemia (K562), leukemia (HL60), T lymphoblast-like polymorph cancerous cell line (CCRF-CEM) and acute T-lymphoblastic leukemia (Jurkat)

Pi et al. reported the DNA binding of the germanium complex of compound **1** (**47**) [62]. Compound **47** showed an increase in fluorescence emission by 46% (at 550 nm) while that of the free parent **1** showed insignificant increase by 8% (at 536 nm). Intercalation with DNA was also confirmed by a UV absorption method through the hypochromism of complex **47** upon addition of CT-DNA. The anti-proliferative evaluationof **47** on the HepG2 cell line (**Table 6**) was followed by AFM that showed deformation of HepG2 cells and increase in the size of cell membrane particles. The effect on cell cycle, measured by flow cytometry, demonstrated that complex **47** causes cell cycle arrest at the G0/G1 phase.

The ruthenium complexes **48-57** were tested on a number of human cancer cell lines; CH1 (ovarian carcinoma), SW480 (colon carcinoma), and A549 (non-small cell lung carcinoma), human urinary bladder (5637), human large cell lung (LCLC-103H), and human pancreatic carcinoma cell lines (DAN-G) [67, 68]. The most significant anti-proliferative activities were observed on the CH1 cell line with IC_{50} values ranging from 0.89 to 7.9 µM (**Table 6**) [67]. The SW480 cell line also showed high sensitivity to these complexes (IC_{50} from 3.4 - 26 µM) while A549 was the least affected with moderate activities (IC_{50} from 8.6 - 30 µM). Kurzwernhart et al.

attempted to determine the mode of action of complexes **48-57** via CDK2 and topoisomerase IIα inhibition assays as well as flow cytometry cell cycle analysis. Despite showing inhibition of CDK2 comparable with the standard reference roscovitine, CDK2 inhibition was excluded by the authors as a mechanism of action. This is due to miscorrelation with the *in vitro* anti-tumor assay activity pattern and poor influence on the G1/S transition of the cell cycle in which CDK2 is involved. On the other hand, complexes **48-57** showed good inhibition of topoisomerase IIα catalytic activity at ≥ 10 μM, which correlated well with the cytotoxic activity (compounds with lowest IC_{50} in MTT assay showed the highest topoisomerase IIα inhibition).

Compounds **61-63** showed promising IC_{50} values on the patient derived (not-established) melanoma cell lines (DMBC11 and DMBC12) as shown in table 6 [61]. Only complex **63** exhibited potency on both DMABC11 and DMBC12 cell lines (IC_{50} = 2.53 and 4.14 μM, respectively). Singh et al. developed four flavonoid ruthenium DMSO complexes (**64-67**) and tested their anti-proliferative activities on the MCF-7 cell line (**Table 6**) in addition to their action on different phases of the cell cycle [63]. Both the free ligands, and their ruthenium complexes, showed similar activities with complex **64** being the most potent with IC_{50} = 16 μM. Analysis of the cell cycle showed that compound **64** dramatically increased the G1 phase and decreased the S phase which might be explained by G1 arrest via inhibition of DNA synthesis in the S phase.

Kostova et al. tested the cytotoxicity of three metal complexes (Cerium, lanthanum and neodymium) with a bis-coumarin (**19**) [75]. Only the cerium complex demonstrated promising anti-proliferative effect on the HL-60 cell line (**Table 6**).

Among four ferrocenylvinyl-flavone derivatives synthesized by Kowalski et al., compound **69** was the most potent (**Table 6**) [41]. The mechanism of action was induction of apoptosis and necrosis as shown by double staining of cells with Hoechst 33258 and propidium iodide. Although anti-tumor activity was evaluated on four human cancer cell lines (HepG2, MCF-7, MDA-MB-231 and CCRF-CEM), CCRF-CEM was the only affected cell line.

Janka and his colleagues also developed a number of ferrocenyl chalcones of which compound **70** showed high activity on Jurkat cell line with IC_{50} = 2.97 μM (**Table 6**) [91]. Complex **71** has an additional ferrocenyl-vinyl group in its structure, however, it didn't show increase in the

activity on the HeLa cell line (IC_{50} = 7.4 μM) when compared with complex **70** (IC_{50} = 7.23 μM).

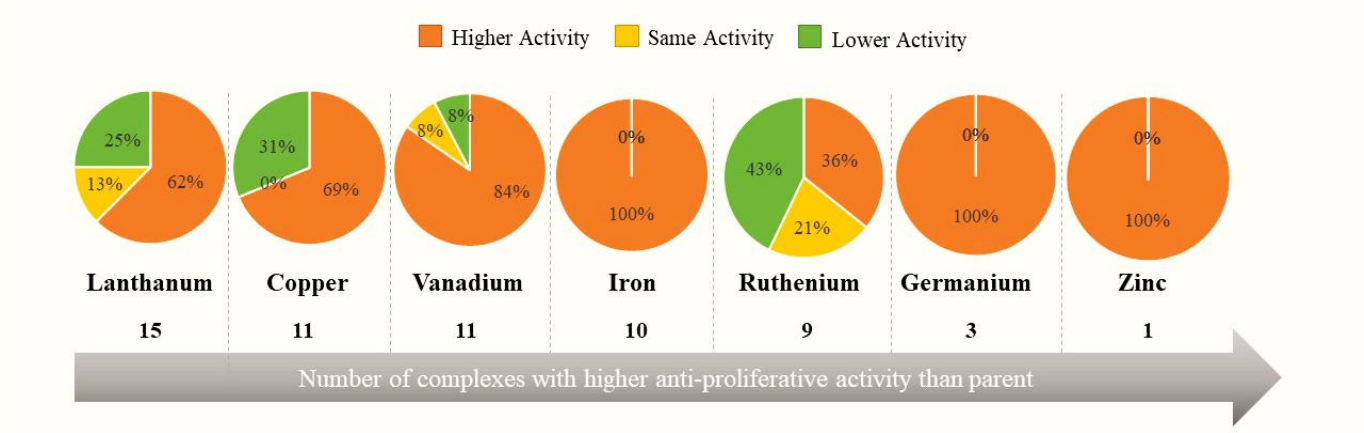

Figure 11. Summary of the effect of chelating different metals on the anti-proliferative activities of parent flavonoids

It can be deduced from **Figure 11** that 64% of the complexes showed enhanced anti-proliferative activities when compared to their parents while 11% maintained the same activity and 25% had lower activity. It should be noted that not all of the complexes' activities were compared to their respective parent flavonoid, depending on the availability of data. All of iron, zinc and germanium complexes showed higher activity than the free flavonoids. However, the total number of zinc complexes is too low to establish a clear view on the effect of complexation. On the other hand, 84%, 69% and 62% of the vanadium, copper and lanthanum complexes, respectively, exhibited better anti-proliferative activities than the free flavonoid. Ruthenium metal complexes showed inconsistent results as 36% showed enhanced activity while 21% had the same activity and 43% showed lower activities than their parent flavonoids.

Future perspectives

Flavonoids have gained significant interest from researches since the early times. This is due to their therapeutic activities in a broad range of fields alongside their natural abundance, with the anti-oxidant and anti-cancer effects of flavonoids being of the greatest impact. Consequently, flavonoids like quercetin and flavopiridol have reached clinical trials as anti-cancer agents. However, none of them are available on the market as anti-cancer drugs due to their poor

pharmacokinetic profiles. The structural ability of flavonoids to coordinate with metal atoms has provided a new strategy for the development of flavonoid metal complexes with better pharmacological profiles. Although chelation of flavonoids with metals enhanced the anti-oxidant and anti-proliferative activities of their free parents in the majority of cases reported herein, more research is needed to confirm if this is a predictable and general phenomenon. Additionally, more research is required to probe whether this enhancement of activity is sufficient to afford new drugs that offer enhanced clinical outcomes when compared to drugs present in the market for the same indications. Larger scale studies probing the impact of complexing different metal atoms with sets of structurally similar and/or different flavonoids on anti-oxidant and anti-proliferative activities are therefore greatly needed. This would pave the way for a better understanding of their structural activity relationships. Furthermore, the use of computational studies like molecular modelling and quantitative SAR (QSAR) can provide valuable information about possible targets and mechanisms of action of these complexes. This will in turn lead to well informed and targeted structural designs.

Executive summary

Introduction

- Flavonoids are polyphenolic compounds with a C_6-C_3-C_6 ring system.
- Flavopiridol, silibinin and quercetin flavonoids have reached clinical trials as anti-cancer agents for various tumors.
- Flavonoids have poor pharmacokinetic properties which limit their clinical applications.
- Flavonoids have the ability to form metal complexes that can change their pharmacological and pharmacokinetic properties.

Synthesis and characterization of flavonoid metal complexes

- Flavonoid metal complexes are synthesized by reacting alcoholic or aqueous solutions of both the flavonoid and the metal under stirring and/or heating conditions.
- Structural characterization techniques of flavonoid metal complexes are versatile and are often complementary to one another.

Anti-oxidant activities of flavonoid metal complexes

- Flavonoid metal complexes demonstrate better radical scavenging activities than their free parents.
- Anti-oxidant activity is measured by the ability to scavenge free radicals like $DPPH^{\cdot}$, $ABTS^{+}$, H_2O_2, $OH^{\cdot}$ and $O_2^{-\cdot}$ in addition to measuring SOD like activity.

- Some flavonoid metal complexes showed DPPH· scavenging activity higher or comparable to vitamin C.

Cytotoxic activities of flavonoid metal complexes

- The discovery of cisplatin had an important role in directing researchers' focus on the development of metal based drugs.
- Flavonoid metal complexes showed promising results on various human cancer cell lines.
- Cytotoxic activity of flavonoid metal complexes is caused by induction of apoptosis and/or oxidative damage of DNA.
- 64% of the flavonoid metal complexes showed better anti-proliferative activities than their parents, 11% maintained the same activity and 25% had lower activity.

Financial disclosure

MK is grateful to the Newton-Mosharafa Fund for a scholarship that has funded her PhD studies.

References

1. Isoda H, Motojima H, Onaga S, Samet I, Villareal MO, Han J. Analysis of the erythroid differentiation effect of flavonoid apigenin on K562 human chronic leukemia cells. *Chem. Biol. Interact.* 220, 269-277 (2014).

2. Perez-Vizcaino F, Fraga CG. Research trends in flavonoids and health. *Arch. Biochem. Biophys.* 646, 107-112 (2018).

3. Wang T-Y, Li Q, Bi K-S. Bioactive flavonoids in medicinal plants: Structure, activity and biological fate. *Asian J. Pharm. Clin. Res.* 13(1), 12-23 (2018).

4. Jeong HJ, Ryu YB, Park S-J *et al.* Neuraminidase inhibitory activities of flavonols isolated from Rhodiola rosea roots and their in vitro anti-influenza viral activities. *Bioorg. Med. Chem.* 17(19), 6816-6823 (2009).

5. Kwon H-J, Kim H-H, Ryu YB *et al.* In vitro anti-rotavirus activity of polyphenol compounds isolated from the roots of Glycyrrhizauralensis. *Bioorg. Med. Chem.* 18(21), 7668-7674 (2010).

6. Sithisarn P, Michaelis M, Schubert-Zsilavecz M, Cinatl Jr J. Differential antiviral and anti-inflammatory mechanisms of the flavonoids biochanin A and baicalein in H5N1 influenza A virus-infected cells. *Antivir. Res.* 97(1), 41-48 (2013).

7. Guz NR, Stermitz FR, Johnson JB *et al.* Flavonolignan and Flavone Inhibitors of a Staphylococcus a ureus Multidrug Resistance Pump: Structure− Activity Relationships. *J. Med. Chem.* 44(2), 261-268 (2001).

8. Kim YS, Ryu YB, Curtis-Long MJ *et al.* Flavanones and rotenoids from the roots of Amorpha fruticosa L. that inhibit bacterial neuraminidase. *Food Chem. Toxicol.* 49(8), 1849-1856 (2011).

9. Ohemeng K, Schwender C, Fu K, Barrett J. DNA gyrase inhibitory and antibacterial activity of some flavones (1). *Bioorg. Med. Chem. Lett.* 3(2), 225-230 (1993).

10. Wu T, He M, Zang X *et al.* A structure–activity relationship study of flavonoids as inhibitors of E. coli by membrane interaction effect. *Biochim. Biophys. Acta (BBA)-Biomembr.* 1828(11), 2751-2756 (2013).

11. Eghorn LF, Hoestgaard-Jensen K, Kongstad KT *et al.* Positive allosteric modulation of the GHB high-affinity binding site by the GABAA receptor modulator monastrol and the flavonoid catechin. *Eur. J. Pharmacol.* 740, 570-577 (2014).

12. Gopinath K, Sudhandiran G. Naringin modulates oxidative stress and inflammation in 3-nitropropionic acid-induced neurodegeneration through the activation of nuclear factor-erythroid 2-related factor-2 signalling pathway. *Neuroscience.* 227, 134-143 (2012).

13. Spencer JP, Vafeiadou K, Williams RJ, Vauzour D. Neuroinflammation: modulation by flavonoids and mechanisms of action. *Mol. Aspects Med.* 33(1), 83-97 (2012).

14. Guo L, Hu W-R, Lian J-H *et al.* Anti-hyperlipidemic properties of CM108 (a flavone derivative) in vitro and in vivo. *Eur. J. Pharmacl.* 551(1-3), 80-86 (2006).

15. Li G, Zhu Y, Zhang Y, Lang J, Chen Y, Ling W. Estimated daily flavonoid and stilbene intake from fruits, vegetables, and nuts and associations with lipid profiles in Chinese adults. *J. Acad. Nutr. Diet.* 113(6), 786-794 (2013).

16. Greeff J, Joubert J, Malan SF, Van Dyk S. Antioxidant properties of 4-quinolones and structurally related flavones. *Bioorg. Med. Chem.* 20(2), 809-818 (2012).

17. Hyun J, Woo Y, Hwang D-S *et al.* Relationships between structures of hydroxyflavones and their antioxidative effects. *Bioorg. Med. Chem. Lett.* 20(18), 5510-5513 (2010).

18. Xie P-J, Huang L-X, Zhang C-H, Zhang Y-L. Phenolic compositions, and antioxidant performance of olive leaf and fruit (Olea europaea L.) extracts and their structure–activity relationships. *J. Funct. Foods.* 16, 460-471 (2015).

19. Ravishankar D, Rajora AK, Greco F, Osborn HM. Flavonoids as prospective compounds for anti-cancer therapy. *Int. J. Biochem. Cell. Biol.* 45(12), 2821-2831 (2013).

20. Ravishankar D, Watson KA, Greco F, Osborn HM. Novel synthesised flavone derivatives provide significant insight into the structural features required for enhanced anti-proliferative activity. *RSC Adv.* 6(69), 64544-64556 (2016).

21. Liu-Smith F, Meyskens FL. Molecular mechanisms of flavonoids in melanin synthesis and the potential for the prevention and treatment of melanoma. *Mol. Nutr. Food Res.* 60(6), 1264-1274 (2016).

22. Klimaszewska-Wiśniewska A, Hałas-Wiśniewska M, Izdebska M, Gagat M, Grzanka A, Grzanka D. Antiproliferative and antimetastatic action of quercetin on A549 non-small cell lung cancer cells through its effect on the cytoskeleton. *Acta Histochem.* 119(2), 99-112 (2017).

23. Mirossay L, Varinská L, Mojžiš J. Antiangiogenic effect of flavonoids and chalcones: An update. *Int. J. Mol. Sci.* 19(1), 27 (2017).

24. Ravishankar D, Watson KA, Boateng SY, Green RJ, Greco F, Osborn HM. Exploring quercetin and luteolin derivatives as antiangiogenic agents. *Eur. J. Med. Chem.* 97, 259-274 (2015).

25. Senderowicz AM. Flavopiridol: the first cyclin-dependent kinase inhibitor in human clinical trials. *Invest. New Drugs.* 17(3), 313-320 (1999).

26. A Study of Venetoclax and Alvocidib in Patients With Relapsed/Refractory Acute Myeloid Leukemia https://ClinicalTrials.gov/show/NCT03441555 (April, 22).

27. Loguercio C, Festi D. Silybin and the liver: from basic research to clinical practice. *World J Gastroenterol.* 17(18), 2288 (2011).

28. A Phase II Study to Assess Efficacy of Combined Treatment With Erlotinib (Tarceva) and Silybin-phytosome (Siliphos) in Patients With EGFR Mutant Lung Adenocarcinoma https://ClinicalTrials.gov/show/NCT02146118 (May, 23).

29. Ferry DR, Smith A, Malkhandi J *et al.* Phase I clinical trial of the flavonoid quercetin: pharmacokinetics and evidence for in vivo tyrosine kinase inhibition. *Clin. Cancer Res.* 2(4), 659-668 (1996).

30. Effect of Quercetin on Green Tea Polyphenol Uptake in Prostate Tissue From Patients With Prostate Cancer Undergoing Surgery https://ClinicalTrials.gov/show/NCT01912820 (May, 7).

31. Mulholland P, Ferry D, Anderson D *et al.* Pre-clinical and clinical study of QC12, a water-soluble, pro-drug of quercetin. *Ann. Oncol.* 12(2), 245-248 (2001).

32. Wu J-W, Lin L-C, Hung S-C, Chi C-W, Tsai T-H. Analysis of silibinin in rat plasma and bile for hepatobiliary excretion and oral bioavailability application. *J. Pharmaceut. Biomed. Anal.* 45(4), 635-641 (2007).

33. Deep A, Marwaha RK, Marwaha MG, Nandal R, Sharma AK. Flavopiridol as cyclin dependent kinase (CDK) inhibitor: a review. *New J. Chem.* 42(23), 18500-18507 (2018).

34. Gugler R, Leschik M, Dengler H. Disposition of quercetin in man after single oral and intravenous doses. *Eur. J. Clin. Pharmacol.* 9(2-3), 229-234 (1975).

35. Samsonowicz M, Regulska E, Kalinowska M. Hydroxyflavone metal complexes-molecular structure, antioxidant activity and biological effects. *Chem. Biol. Interact.* 273, 245-256 (2017).

** This article reviews the synthetic procedures, spectroscopic properties, biological activities and mechanisms of action of hydroxyflavone metal complexes.

36. Kasprzak MM, Szmigiero L, Zyner E, Ochocki J. Proapoptotic activity in vitro of two novel ruthenium (II) complexes with flavanone-based ligands that overcome cisplatin resistance in human bladder carcinoma cells. *J. Inorg. Biochem.* 105(4), 518-524 (2011).

37. Kasprzak MM, Erxleben A, Ochocki J. Properties and applications of flavonoid metal complexes. *RSC Adv.* 5(57), 45853-45877 (2015).

** This review discusses the different metal coordination patterns, structural properties and the various applications of flavonoid metal complexes.

38. Grazul M, Budzisz E. Biological activity of metal ions complexes of chromones, coumarins and flavones. *Coord. Chem. Rev.* 253(21-22), 2588-2598 (2009).

* This review gives details about the mechanisms of action of some metals and flavonoid metal complexes in the treatment of several pathological conditions.

39. Monserrat J-P, Tiwari KN, Quentin L *et al.* Ferrocenyl flavonoid-induced morphological modifications of endothelial cells and cytotoxicity against B16 murine melanoma cells. *J. Organomet. Chem.* 734, 78-85 (2013).

40. Tiwari KN, Monserrat J-P, Hequet A *et al.* In vitro inhibitory properties of ferrocene-substituted chalcones and aurones on bacterial and human cell cultures. *Dalton Trans.* 41(21), 6451-6457 (2012).

41. Kowalski K, Koceva-Chyła A, Szczupak Ł *et al.* Ferrocenylvinyl-flavones: Synthesis, structure, anticancer and antibacterial activity studies. *J. Organomet. Chem.* 741, 153-161 (2013).

42. Wang B-D, Yang Z-Y, Wang Q, Cai T-K, Crewdson P. Synthesis, characterization, cytotoxic activities, and DNA-binding properties of the La (III) complex with Naringenin Schiff-base. *Bioorg. Med. Chem.* 14(6), 1880-1888 (2006).

43. Tabassum S, Zaki M, Afzal M, Arjmand F. New modulated design and synthesis of quercetin–Cu II/Zn II–Sn 2 IV scaffold as anticancer agents: in vitro DNA binding profile, DNA cleavage pathway and Topo-I activity. *Dalton Trans.* 42(27), 10029-10041 (2013).

* This article offers the novel synthesis of bimetallic quercetin complexes. It provides a detailed explanation of their anti-cancer mechanism of action supported by the relevant biological assays and computational studies.

44. Ciesielska E, Studzian K, Zyner E, Ochocki J, Szmigiero L. DNA damage and apoptosis induction in L1210 cells by cis-diamminedichloroplatinum (II) and its new aminoflavone analogue. *Cellular Mol. Biol. Lett.* 5(2), 235-235 (2000).

45. Weil JA, Bolton JR. *Electron paramagnetic resonance: elementary theory and practical applications*. John Wiley & Sons, (2007).

46. Etcheverry SB, Ferrer EG, Naso L, Rivadeneira J, Salinas V, Williams PaM. Antioxidant effects of the VO (IV) hesperidin complex and its role in cancer chemoprevention. *J. Biol. Inorg. Chem.* 13(3), 435 (2008).

47. Naso LG, Ferrer EG, Butenko N *et al.* Antioxidant, DNA cleavage, and cellular effects of silibinin and a new oxovanadium (IV)/silibinin complex. *J. Biol. Inorg. Chem.* 16(4), 653-668 (2011).

48. Naso LG, Lezama L, Rojo T *et al.* Biological evaluation of morin and its new oxovanadium (IV) complex as antio-xidant and specific anti-cancer agents. *Chem Biol Interact.* 206(2), 289-301 (2013).

49. Naso LG, Lezama L, Valcarcel M *et al.* Bovine serum albumin binding, antioxidant and anticancer properties of an oxidovanadium (IV) complex with luteolin. *J. Inorg. Biochem.* 157, 80-93 (2016).

50. Jurd L, Geissman T. Absorption spectra of metal complexes of flavonoid compounds. *J. Org. Chem.* 21(12), 1395-1401 (1956).

51. Selvaraj S, Krishnaswamy S, Devashya V, Sethuraman S, Krishnan UM. Flavonoid–metal ion complexes: a novel class of therapeutic agents. *Med. Res. Rev.* 34(4), 677-702 (2014).

* This review summarizes the structural characterization techniques and biological significance of flavonoid metal complexes.

52. Ren J, Meng S, Lekka CE, Kaxiras E. Complexation of flavonoids with iron: structure and optical signatures. *J. Phys. Chem. B.* 112(6), 1845-1850 (2008).

53. Tan J, Wang B, Zhu L. DNA binding and oxidative DNA damage induced by a quercetin copper (II) complex: potential mechanism of its antitumor properties. *J. Biol. Inorg. Chem.* 14(5), 727-739 (2009).

54. Tan J, Zhu L, Wang B. DNA binding and cleavage activity of quercetin nickel (II) complex. *Dalton Trans.* (24), 4722-4728 (2009).

55. Zhou J, Wang L-F, Wang J-Y, Tang N. Synthesis, characterization, antioxidative and antitumor activities of solid quercetin rare earth (III) complexes. *J. Inorg. Biochem.* 83(1), 41-48 (2001).

56. Etcheverry SB, Barrio DA, Williams PA, Baran EJ. On the interaction of the vanadyl (IV) cation with lactose. *Biol. Trace. Elem. Res.* 84(1-3), 227-238 (2001).

57. Zeng Y-B, Yang N, Liu W-S, Tang N. Synthesis, characterization and DNA-binding properties of La (III) complex of chrysin. *J. Inorg. Biochem.* 97(3), 258-264 (2003).

58. Naso L, Ferrer EG, Lezama L, Rojo T, Etcheverry SB, Williams P. Role of oxidative stress in the antitumoral action of a new vanadyl (IV) complex with the flavonoid chrysin in two osteoblast cell lines: relationship with the radical scavenger activity. *J. Biol. Inorg. Chem.* 15(6), 889-902 (2010).

59. Wang Q, Zhao L, Zhao H *et al.* Complexation of luteolin with lead (II): Spectroscopy characterization and theoretical researches. *J. Inorg. Biochem.* 193, 25-30 (2019).

60. Kostova I, Manolov I, Nicolova I, Konstantinov S, Karaivanova M. New lanthanide complexes of 4-methyl-7-hydroxycoumarin and their pharmacological activity. *Eur. J. Med. Chem.* 36(4), 339-347 (2001).

61. Pastuszko A, Majchrzak K, Czyz M, Kupcewicz B, Budzisz E. The synthesis, lipophilicity and cytotoxic effects of new ruthenium (II) arene complexes with chromone derivatives. *J. Inorg. Biochem.* 159, 133-141 (2016).

62. Pi J, Zeng J, Luo J-J, Yang P-H, Cai J-Y. Synthesis and biological evaluation of Germanium (IV)–polyphenol complexes as potential anti-cancer agents. *Bioorg. Med. Chem. Lett.* 23(10), 2902-2908 (2013).

63. Singh AK, Saxena G, Arshad M. Synthesis, characterization and biological evaluation of ruthenium flavanol complexes against breast cancer. *Spectrochim. Acta A Mol. Biomol. Spectrosc.* 180, 97-104 (2017).

64. Tu L-Y, Pi J, Jin H, Cai J-Y, Deng S-P. Synthesis, characterization and anticancer activity of kaempferol-zinc (II) complex. *Bioorg. Med. Chem. Lett.* 26(11), 2730-2734 (2016).

65. Roy S, Mallick S, Chakraborty T *et al.* Synthesis, characterisation and antioxidant activity of luteolin–vanadium (II) complex. *Food Chem.* 173, 1172-1178 (2015).

66. Tan M, Zhu J, Pan Y *et al.* Synthesis, cytotoxic activity, and DNA binding properties of copper (II) complexes with hesperetin, naringenin, and apigenin. *Bioinorg. Chem. Appl.* 2009, (2009).

67. Kurzwernhart A, Kandioller W, BäChler S *et al.* Structure–activity relationships of targeted RuII (η6-p-Cymene) anticancer complexes with flavonol-derived ligands. *J. Med. Chem.* 55(23), 10512-10522 (2012).

68. Kurzwernhart A, Kandioller W, Bartel C *et al.* Targeting the DNA-topoisomerase complex in a double-strike approach with a topoisomerase inhibiting moiety and covalent DNA binder. *Chem. Commun.* 48(40), 4839-4841 (2012).

69. Yang F, Jin H, Pi J *et al.* Anti-tumor activity evaluation of novel chrysin–organogermanium (IV) complex in MCF-7 cells. *Bioorg. Med. Chem. Lett.* 23(20), 5544-5551 (2013).

70. Dong H, Yang X, He J, Cai S, Xiao K, Zhu L. Enhanced antioxidant activity, antibacterial activity and hypoglycemic effect of luteolin by complexation with manganese (II) and its inhibition kinetics on xanthine oxidase. *RSC Adv.* 7(84), 53385-53395 (2017).

71. Pereira R, Andrades NE, Paulino N *et al.* Synthesis and characterization of a metal complex containing naringin and Cu, and its antioxidant, antimicrobial, antiinflammatory and tumor cell cytotoxicity. *Molecules.* 12(7), 1352-1366 (2007).

72. Manolov I, Kostova I, Konstantinov S, Karaivanova M. Synthesis, physicochemical characterization and cytotoxic screening of new complexes of cerium, lanthanum and neodymium with Niffcoumar sodium salt. *Eur. J. Med. Chem.* 34(10), 853-858 (1999).

73. Kostova I, Manolov I, Karaivanova M. Synthesis, physicochemical characterization, and cytotoxic screening of new zirconium complexes with coumarin derivatives. *Arch. Pharm.* 334(5), 157-162 (2001).

74. Pastuszko A, Niewinna K, Czyz M, Jóźwiak A, Małecka M, Budzisz E. Synthesis, X-ray structure, electrochemical properties and cytotoxic effects of new arene ruthenium (II) complexes. *J. Organomet. Chem.* 745, 64-70 (2013).

75. Kostova I, Kostova R, Momekov G, Trendafilova N, Karaivanova M. Antineoplastic activity of new lanthanide (cerium, lanthanum and neodymium) complex compounds. *J. Trace Elem. Med. Biol.* 18(3), 219-226 (2005).

76. Leon IE, Di Virgilio AL, Porro V *et al.* Antitumor properties of a vanadyl (IV) complex with the flavonoid chrysin [VO (chrysin) 2 EtOH] 2 in a human osteosarcoma model: the role of oxidative stress and apoptosis. *Dalton Trans.* 42(33), 11868-11880 (2013).

77. Chen Y-H, Yang Z-S, Wen C-C *et al.* Evaluation of the structure–activity relationship of flavonoids as antioxidants and toxicants of zebrafish larvae. *Food Chem.* 134(2), 717-724 (2012).

78. Rice-Evans CA, Miller NJ, Paganga G. Structure-antioxidant activity relationships of flavonoids and phenolic acids. *Free Radic. Biol. Med.* 20(7), 933-956 (1996).

* This review compares the anti-oxidant potential of a range of flavonoid structures giving a detailed idea about the impact of each functional group on the anti-oxidant activity

79. Pietta P-G. Flavonoids as antioxidants. *J. Na.t Prod.* 63(7), 1035-1042 (2000).

80. Rosenberg B, Vancamp L, Trosko JE, Mansour VH. Platinum compounds: a new class of potent antitumour agents. *Nature.* 222(5191), 385 (1969).

81. Jung Y, Lippard SJ. Direct cellular responses to platinum-induced DNA damage. *Chem. Rev.* 107(5), 1387-1407 (2007).

82. Pil P. Cisplatin and related drugs. *Encyclopedia of Cancer.* 1, 391-410 (1997).

83. Fuertes MA, Alonso C, Pérez JM. Biochemical modulation of cisplatin mechanisms of action: enhancement of antitumor activity and circumvention of drug resistance. *Chem. Rev.* 103(3), 645-662 (2003).

84. Tan J, Zhu L, Wang B. From GC-rich DNA binding to the repression of survivin gene for quercetin nickel (II) complex: implications for cancer therapy. *Biometals.* 23(6), 1075-1084 (2010).

85. Kaizer J, Baráth G, Pap J, Speier G, Giorgi M, Réglier M. Manganese and iron flavonolates as flavonol 2, 4-dioxygenase mimics. *Chem. Commun.* (48), 5235-5237 (2007).

86. Sahu SC, Gray GC. Interactions of flavonoids, trace metals, and oxygen: nuclear DNA damage and lipid peroxidation induced by myricetin. *Cancer Lett.* 70(1-2), 73-79 (1993).

87. León I, Cadavid-Vargas J, Tiscornia I *et al.* Oxidovanadium (IV) complexes with chrysin and silibinin: anticancer activity and mechanisms of action in a human colon adenocarcinoma model. *J. Biol. Inorg. Chem.* 20(7), 1175-1191 (2015).

88. Naruse T, Nishida Y, Ishiguro N. Synergistic effects of meloxicam and conventional cytotoxic drugs in human MG-63 osteosarcoma cells. *Biomed. Pharmacother.* 61(6), 338-346 (2007).

89. León IE, Díez P, Etcheverry SB, Fuentes M. Deciphering the effect of an oxovanadium (IV) complex with the flavonoid chrysin (VOChrys) on intracellular cell signalling pathways in an osteosarcoma cell line. *Metallomics.* 8(8), 739-749 (2016).

90. Yang F, Gong L, Jin H *et al.* Chrysin–organogermanium (IV) complex induced Colo205 cell apoptosis-associated mitochondrial function and anti-angiogenesis. *Scanning.* 37(4), 246-257 (2015).

91. Janka V, Žatko D, Ladislav V, Pál P, Janka P, Gabriela M. Some ferrocenyl chalcones as useful candidates for cancer treatment. *In Vitro Cell. Dev. Biol. Anim.* 51(9), 964-974 (2015).